CENTRO INTERNACIONAL DE ESTUDOS
DE DOUTORAMENTO E AVANZADOS
DA USC (CIEDUS)

TESIS DE DOCTORADO

THERMOPHYSICAL CHARACTERIZATION OF LUBRICANTS ADDITIVATED WITH NANOPARTICLES FOR THEIR APPLICATION IN RENEWABLE ENERGIES

María Jesús García Guimarey

ESCUELA DE DOCTORADO INTERNACIONAL

PROGRAMA DE DOCTORADO EN CIENCIA DE MATERIALES

SANTIAGO DE COMPOSTELA

AÑO 2019

USC
UNIVERSIDADE
DE SANTIAGO
DE COMPOSTELA

DECLARACIÓN DEL AUTOR DE LA TESIS

Thermophysical Characterization of Lubricants Additivated with Nanoparticles for their Application in Renewable Energies

Dña. María Jesús García Guimarey

Presento mi tesis, siguiendo el procedimiento adecuado al Reglamento, y declaro que:

1) La tesis abarca los resultados de la elaboración de mi trabajo.

2) En su caso, en la tesis se hace referencia a las colaboraciones que tuvo este trabajo.

3) La tesis es la versión definitiva presentada para su defensa y coincide con la versión enviada en formato electrónico.

4) Confirmo que la tesis no incurre en ningún tipo de plagio de otros autores ni de trabajos presentados por mí para la obtención de otros títulos.

En Santiago de Compostela, 11 de abril. de 2019

Fdo. María Jesús García Guimarey

USC
UNIVERSIDADE
DE SANTIAGO
DE COMPOSTELA

AUTORIZACIÓN DE LOS DIRECTORES DE LA TESIS

Thermophysical Characterization of Lubricants Additivated with Nanoparticles for their Application in Renewable Energies

Dª. María José Pérez Comuñas

D. Alfredo José Amigo Pombo

INFORMAN:

Que la presente tesis, se corresponde con el trabajo realizado por Dª. ***María Jesús García Guimarey****, bajo nuestra dirección, y autorizamos su presentación, considerando que reúne los requisitos exigidos en el Reglamento de Estudios de Doctorado de la USC, y que como directores de esta no incurre en las causas de abstención establecidas en la Ley 40/2015.*

De acuerdo con el artículo 41 del Reglamento de Estudios de Doctorado, declaramos también que la presente tesis doctoral es idónea para ser defendida en base a la modalidad de COMPENDIO DE PUBLICACIONES, en los que la participación de la doctoranda fue decisiva para su elaboración.

La utilización de estos artículos en esta memoria, está en conocimiento de los coautores, tanto doctores como no doctores. Además, estos últimos tienen conocimiento de que ninguno de los trabajos aquí reunidos podrá ser presentado en ninguna otra tesis doctoral.

En Santiago de Compostela, 11 de abril de 2019

Fdo. María José Pérez Comuñas

Fdo. Alfredo José Amigo Pombo

USC
UNIVERSIDADE
DE SANTIAGO
DE COMPOSTELA

Agradecimientos

Me gustaría agradecer el constante apoyo que he recibido, tanto profesional como personal, a lo largo de la realización de esta Tesis Doctoral por parte de mis directores, la Prof. María José Pérez Comuñas y el Prof. Alfredo José Amigo Pombo. Sin vuestra orientación y transmisión de conocimientos este trabajo no habría sido posible. En especial a mi tutora María, por su paciencia, por su gran organización, por su comprensión y por las incontables horas que me ha dedicado.

A la Prof. Josefa Fernández por haberme dado la oportunidad de embarcarme en este proyecto y a la Prof. Enriqueta López, porque sin serlo también ha ejercido de tutora, le agradezco toda la ayuda proporcionada, ya que parte de este trabajo es mérito suyo.

Al Ministerio de Economía y Empresa de España y al Fondo Europeo de Desarrollo Regional (FEDER) por financiar los proyectos en los que se enmarca esta Tesis Doctoral y al programa IACOBUS por la financiación concedida para realizar la estancia en la Universidad de Porto (Portugal).

I want to thank Prof. Seabra, Drs. David Gonçalves and Carlos Fernandes and their research group (Pedro, Beatriz and Ramiro) from the Faculdade de Engenharia da Universidade do Porto (FEUP) and the Institute of Science and Innovation in Mechanical and Industrial Engineering (INEGI) for their support and guidance during my research stay in Porto. También, a Marina y a Natalia no sólo por haberme enseñado a disfrutar de Oporto, sino porque sin casi conocerme, me hicieron sentir como en casa.

Al grupo NaFoMat, y en especial, a María V. y a Pepi, porque han sido unas compañeras extraordinarias, que han estado a mi lado en todo momento. Los cafés y las clases de zumba sin ellas no hubiesen sido lo mismo. A María Herrero por su colaboración con el perfilómetro y por su grata compañía. Al equipo Boom (Jujo, Damián y Sema) por su gran sentido del humor y por los infinitos momentos de risas que me han regalado.

Al Prof. Luis Lugo y a los Drs. David C. y Javi V. por su calurosa acogida durante mi estancia en la Universidad de Vigo, por todo lo que me han ayudado y porque ha sido un placer trabajar con ellos.

A Aarón y a Sema porque han sido mis dos grandes apoyos día a día durante estos tres años, gracias por ser mis amigos y saber quitarme una sonrisa cuando más lo necesitaba. A Miguel y a Manuel porque su esfuerzo y generosidad han permitido completar esta Tesis. A Mónica y a Félix, porque han sido unos estupendos compañeros de viaje. A Conchi por hacerme las largas tardes tan amenas, por sus buenos consejos y por ser tan auténtica.

A Mateo Mundito y a Pablo Malpica que han estado presentes desde mis inicios en el doctorado, gracias por las agradables conversaciones y por las risas de pasillo.

A María G., Albita, Tomy y Adri (mis BioVips) por estar siempre a mi lado y por estar siempre disponibles cuando tanto necesitaba unas cañas. Santiago no hubiera sido lo mismo sin vosotros, y lo sabéis.

A todos mis amigos (Julieta, Fátima, Sara, Lara, Xio, Lucía, Kelly, Marta, Pili, Tania Leiro, Dani, Héctor, Aly, Yáñez, Tania Goldar, Antia, Tamy, Paulis) porque cerca o lejos me habéis demostrado que siempre puedo contar con vosotros.

A mis predocs Rita, Lore y Arís por nuestros martes, lunes, o jueves, el día era lo de menos, lo importante era disfrutar de vuestra compañía.

Y por supuesto, a mi familia: a Ana porque además de hermana es amiga y porque solo ella sabe responder cada mañana con una sonrisa a mi mal humor, a mi hermano Jose porque ha sido el instigador de mi faceta investigadora y a mi padre, porque aunque nunca lo sepa, sé que estaría orgulloso. Por último, todo esto no sería posible sin la fortaleza, comprensión y alegría de mi madre. Ella siempre ha sido y será una inspiración.

Gracias a todos y a cada uno de vosotros, por contribuir a que esta Tesis se hiciese realidad.

Abstract

This PhD Thesis is focused on the analysis of thermophysical and tribological properties of base oils (esters, polyalkylene glycols and polyalphaolefins), commercial lubricants (gearbox oil and motor oil) and new formulated nanolubricants. Nanoparticles of different morphology (spherical, rod-like and laminar) have been used as lubricant additives: zirconium oxide and boron nitride nanoparticles and graphene nanoplatelets. Installation and star-up of different technical apparatus have been performed to characterize the base oils and the nanoadditives, to prepare the nanolubricants, and to control the temporal stability, the sedimentation rate and the aggregation level.

In order to propose new potential lubricants is of vital importance to analyse the effect that the addition of the nanoadditives has on their thermophysical properties, because they affect the final lubricants performance. With this aim, the volumetric and viscous behaviour, viscosity index, flow curves and thermal conductivity of base oils, commercial lubricants and nanolubricants were experimentally determined. Several scientific techniques were used: atmospheric and high pressure vibrating tube densimeters, rotational viscometer, cone-plate geometry rheometer, among others.

For the application of nanolubricants it is also necessary to better know the mechanism that control their tribological performance. In this work we are focused on the pressure-viscosity coefficient for elastohydrodynamic lubrication, film thickness, wear and friction coefficient. These properties were obtained from a high-pressure falling body viscometer, a ball-on-disc apparatus equipped with optical interferometry, a 3D perfilometer and a ball-on-plate configuration tribometer. Finally, the effect of the morphology, size and concentration of the nanoadditives on both the thermophysical and tribological properties was studied.

Keywords: synthetic oils, nanoparticles, thermophysical properties, high pressure, tribological behaviour.

Resumen

Esta Tesis Doctoral se centra en el análisis de las propiedades termofísicas y tribológicas de aceites base (ésteres, polialquilenglicoles y polialfaolefinas), lubricantes comerciales (aceites de caja de engranajes y de motor) y nuevos nanolubricantes formulados. Se han empleado nanopartículas de diferente morfología (esférica, rod-like y laminar) como aditivos lubricantes: nanopartículas de óxido de zirconio y de nitruro de boro y nanoplaquetas de grafeno. Se ha realizado la instalación y puesta en marcha de diferentes equipos para caracterizar los aceites base y los nanoaditivos, para preparar los nanolubricantes y para controlar la estabilidad temporal, la velocidad de sedimentación y el nivel de agregación.

Para poder proponer nuevos potenciales lubricantes es de vital importancia analizar el efecto que tiene la adición de los nanoaditivos sobre sus propiedades termofísicas, ya que éstas afectan al rendimiento del lubricante. Con este objetivo, se ha determinado el comportamiento volumétrico y viscoso, el índice de viscosidad, las curvas de flujo y la conductividad térmica de los aceites base, de los lubricantes comerciales y de los nanolubricantes. Se emplearon distintas técnicas experimentales: densímetros de tubo vibrante a presión atmosférica y a alta presión, viscosímetro rotacional, reómetro con geometría cono-plato, entre otras.

Para la aplicación de los nanolubricantes también es necesario conocer mejor los mecanismos que controlan su comportamiento tribológico. Este trabajo se ha centrado en determinar el coeficiente de viscosidad-presión para lubricación elastohidrodinámica, el espesor de película, el desgaste y el coeficiente de fricción. Estas propiedades se han determinado a partir de un viscosímetro de caída de cuerpo a alta presión, un tribómetro de bola sobre disco equipado con interferometría óptica, un perfilómetro 3D y un tribómetro de configuración bola sobre placa. Finalmente, también se ha estudiado el efecto que tienen la morfología, el tamaño y la concentración de los nanoaditivos sobre las propiedades termofísicas y tribológicas de los nanolubricantes.

Palabras clave: aceites sintéticos, nanopartículas, propiedades termofísicas, alta presión, comportamiento tribológico.

Resumo

Esta Tesis Doutoral céntrase na análise das propiedades termofísicas e tribolóxicas de aceites base (ésteres, polialquilenglicois e polialfaolefinas), lubricantes comerciais (aceites de caixa de engranaxes e de motor) e novos nanolubricantes formulados. Empregáronse nanopartículas de diferente morfoloxía (esférica, rod-like e laminar) como aditivos lubricantes: nanopartículas de óxido de zirconio e de nitruro de boro e nanoplaquetas de grafeno. Realizouse a instalación e posta en marcha de diferente equipamento para caracterizar os aceites base e os nanoaditivos, para preparar os nanolubricantes e para controlar a estabilidade temporal, a velocidade de sedimentación e o nivel de agregación.

Para propor novos potenciais lubricantes é de vital importancia a análise do efecto que ten a adición dos nanoaditivos sobre as súas propiedades termofísicas, xa que ditas propiedades afectan ao rendemento do lubricante. Con este obxectivo, determinouse o comportamento volumétrico e viscoso, o índice de viscosidade, as curvas de fluxo e a condutividade térmica dos aceites base, dos lubricantes comerciais e dos nanolubricantes. Empregáronse diversas técnicas experimentais: densímetros de tubo vibrante a presión atmosférica e a alta presión, viscosímetro rotacional, reómetro con xeometría cono-prato, entre outras.

Para a aplicación dos nanolubricantes tamén é necesario un mellor coñecemento dos mecanismos que controlan o seu comportamento tribolóxico. Este traballo centrouse en determinar o coeficiente de viscosidade-presión para a lubricación elastohidrodinámica, o espesor de película, o desgaste e o coeficiente de fricción. Estas propiedades foron obtidas a partir dun viscosímetro de caída de corpo a alta presión, un tribómetro de bola sobre disco equipado con interferometría óptica, un perfilómetro 3D e un tribómetro de configuración bola sobre placa. Finalmente, tamén se estudiou o efecto que teñen a morfoloxía, o tamaño e a concentración dos nanoaditivos sobre as propiedades termofísicas e tribolóxicas dos nanolubricantes.

Palabras chave: aceites sintéticos, nanopartículas, propiedades termofísicas, alta presión, comportamento tribolóxico.

USC
UNIVERSIDADE
DE SANTIAGO
DE COMPOSTELA

INDEX

USC
UNIVERSIDADE
DE SANTIAGO
DE COMPOSTELA

1. INTRODUCTION

USC
UNIVERSIDADE
DE SANTIAGO
DE COMPOSTELA

1. INTRODUCTION

1.1. Motivation

The worldwide consumption of energy was around 396 10^8 joules in 2014, 29% of this energy is consumed in industrial activity, 28% in transportation, 34% in residential use (domestic, agriculture, among others) and 9% on raw materials [1]. All the processes of obtaining energy, especially mechanical systems, present losses, mainly due to friction and wear. Several studies [1,2] have remarked the impact of tribology (the science and technology of friction, wear and lubrication) on energy consumption. Controlling friction and wear the consumption of energy can be reduced significantly. For instance, around 25% of the energy generated in a fuel combustion engine is lost through friction [3]. Friction reduction means an increase on energy performance and hence, a decrease of emission of greenhouse gases. While wear reduction implies greater reliability and lifetime of mechanical systems reducing waste generated.

Modern machines operate under more severe conditions with more stringent requirements and under the background of the conservation and preservation of natural resources following environmental regulations. Hence, inevitably the future of tribology will be interconnected with technological progress [4]. At this point, the lubrication is of crucial importance [5-7]. The enormous economic effect of controlling and optimizing lubrication, and the importance of lubrication control in tribology is outlined in many investigations [8-10]. Lubricants (substances that reduces friction, heat and wear) are a powerful tool for tribology, thus they perform a number of critical functions: lubrication, cooling, cleaning and suspending, and protecting metal surfaces against corrosive damage [1]. To select the type of lubricant employed, several factors must be taken into account: temperature range, speed, load, materials to be encountered, and general design considerations of the machine itself [11]. An inappropriately selected lubricant may lead to a considerable increase in the operating costs of the machine.

The need to develop new lubricants with improved anti-friction and anti-wear properties are justified by the energetic saving that this would imply. Some of the recent advances on the lubricant formulation was to include nanomaterials as additives due to their especial tribological properties [12-15]. However, application of nanolubricants has several current obstacles such as: their low temporal stability, their high production cost and the need to better knowledge the mechanism that control their tribological performance. To propose new potential lubricants is of vital importance to analyze the effect that the addition

of the nanoadditives has on their thermophysical properties, because they affect also the final lubricants performance. The knowledge of the viscosity and rheological behavior is important in the design and in the prediction of the behavior of a lubricated mechanical system. Moreover, viscosity governs the sealing effect and the consumption rate oil, likewise, optimizes the starting and operating requirements of the machines under conditions of varying temperature. Therefore, a strong alteration of this property may cause failure in the pumping system. Thermal conductivity is essential in assessing heating effect in lubrication and in bearing design. Moreover, due to working pressure existing in the bearings with fluids film lubrication, the change of the density with pressure is essential in highly loaded lubricated contacts.

1.2. Lubricants

Lubricant is a substance used to reduce friction and wear of surfaces in relative motion, such as in gears or bearings. Depending on its nature, lubricants are also used to eliminate heat and wear particles, supply additives into the contact area, transmit power, protect and seal, among others. Essentially, lubricants can perform three main applications: lubrication, cooling and sealing. Different forms between interacting parts as well as different lubrication conditions can happen in lubricated systems. It is important to know how the friction coefficient varies depending on the conditions in which the interaction between the surfaces occurs: lubricant viscosity, η, load, N, and sliding speed, v. Depending on the presence or absence of an external pressure source, four lubrication regimes are identified [16,17]. Figure 1.1 shows the Stribeck curve which classify the regimes according to the applied load and the sliding speed [11].

Under conditions of high load and low speed, the lubricant is displaced from the contact zones and the Boundary Lubrication (BL) takes place. Solid-solid contact occurs, and consequently the friction and wear increase. As the load decreases or the speed increases, the separation between the surfaces increases. Therefore, there comes a time when the load is partially supported by the lubricant and the surface (in contact), this is known as Mixed Lubrication (ML). If the load continues to decrease, a point is reached where there is no direct physical contact between moving parts, at this moment Elastohydrodynamic Lubrication (EHL) takes place. Finally, at lower load or higher speed, the separation between the surfaces is still greater, Hydrodynamic Lubrication (HDL) occurs.

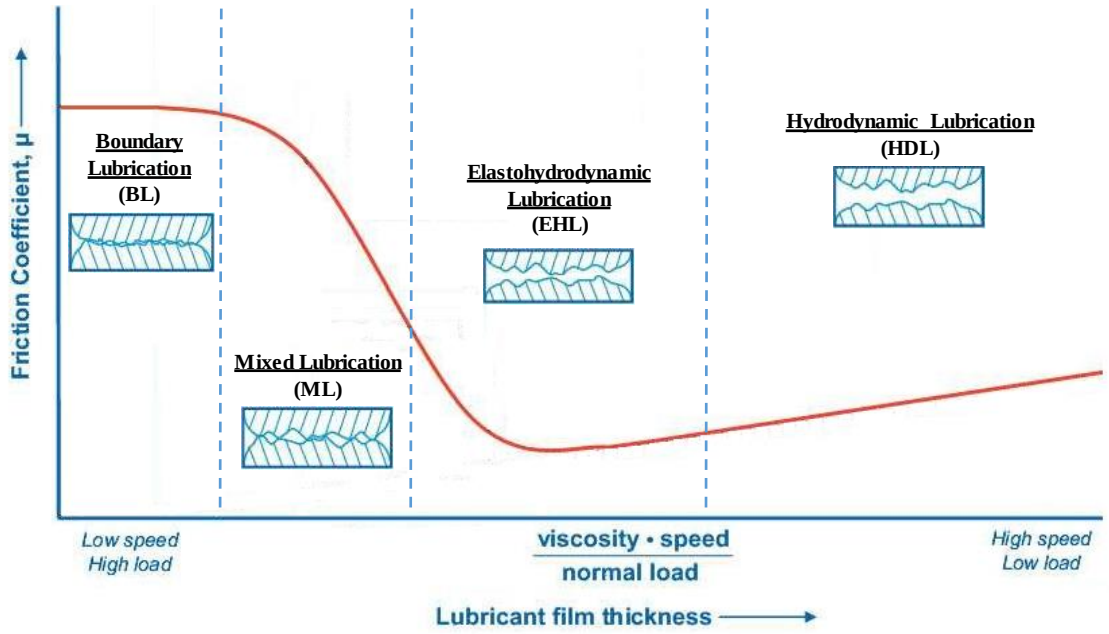

Figure 1.1. Stribeck curve showing the dependence of the friction coefficient with the film thickness [18].

Generally, a lubricant is formulated from base oils with respect to which appropriate additives are selected and properly blended to achieve a delicate balance in performance characteristics of the finished lubricant [2]. Base oils are broadly classified into three categories depending on the obtaining process: mineral, synthetic, and biological oils. Mineral oils [19-21] are manufactured by refining petroleum crude oil (extremely complex mixture of organic chemicals of different molecular size). These oils comprise hydrocarbons with a broad molecular weight ranging from 250 (for low-viscosity lubricants) up to 1000 (for high-viscosity lubricants) [19]. Mineral oils can be classified into paraffinic or naphthenic depending on the chemical structure of the predominant components. Mineral oils are the most widely used fluids for electrical insulation and heat transfer in equipment such as transformers, capacitors and bushings among others [22]. Although mineral oils represent the majority of the market demand (currently around 95% of all lubricants produced are based on mineral oils) because they are cheaper than synthetic oils, many technological advances in equipment and machinery would not be possible without the benefits offered by synthetic oils [20].

The second category in the classification is the synthetic oils, which are obtained by chemical synthesis. The starting reagents can be of both vegetable and mineral nature. Synthetic oils have better characteristics than mineral oils: better behaviour with temperature (the viscosity varies smoothly) and a much lower flow point, which makes them much indicated fluids for low temperature applications. They have better stability against oxidation

so they are equally suitable at high temperatures. The fact that makes them particularly interesting is that it is relatively easy to control the reactions that give rise to these products; hence, their properties can be controlled more strictly by acting on the type of monomers and on the degree of polymerization.

Synthetic lubricants [23] can be mainly classified according to several factors (chemical composition, production process and chemical structure) in polyalphaolefins, trimellitates, polyol esters and polyalkylene glycols. Polyalphaolefins (PAOs) are hydrocarbon polymers manufactured by a catalytic oligomerization of linear alpha-olefins, frequently, 1-decene or a mixture of α-olefins containing, in general, between six to twelve carbon atoms. PAOs are normally classified according to their kinematic viscosity at 373.15 K. The type of catalyst employed determines the degree of kinematic viscosity of the product. Low-kinematic viscosity PAOs (2 to 10 $mm^2.s^{-1}$) are produced by oligomerization catalysed by BF_3, while high-kinematic viscosity PAOs (>10 $mm^2.s^{-1}$) are obtained through Ziegler-Natta or organic chlorides catalysts [20,24,25]. PAOs are considered high-performance lubricants and provide a high viscosity index and hydrolytic stability. PAOs are the most commonly used, and are generally less expensive than other synthetic lubricants, although more than mineral oils. They are mainly used in automotive industry as engine lubricants and gear oils and as base oil for hydraulic oils, automatic transmission oils, compressor/pump oils and greases [26].

Trimellitates [27] are manufactured by esterification of a trimellitic anhydride (TMA) with a monofunctional alcohol. They present a wide viscosity range (ISOVG from 46 to 320). In addition, these fluids stand out by their exceptional thermal stability and resistance to extraction. Due to their high molecular weight they have low volatility that makes them great lubricants. Trimellitates have applications in automobile industry where resistance to high temperature is required and are used in lubricant applications, for instance as greases or compressor oils [20,28]. Polyol esters are also produced from an esterification but in this case, both, alcohol and acid, are multifunctional. Multifunctional alcohol usually contains three or four alcohol groups [29]. Among their main applications highlight: refrigeration air compressors, aviation, metalworking and fire resistant and biodegradable hydraulic fluids [20]. They can also be mixed with PAOs to improve the solubility of the additives package and to reduce the seal shrinkage risk that involves the use of PAOs [30].

Polyalkylene glycols are manufactured by the continued polymerization of alkaline oxide monomers with a nucleophilic starter. The most commonly used alkaline oxides are two types of copolymers: ethylene oxide (EO) and propylene oxide (PO). The nucleophilic

starter is usually an alcohol either a short chain linear alcohol or 2 diol, but also amines or carboxylic acids can be used. Finally, the typical catalysts in this kind of polymerization are alkali-metal hydroxides (sodium or potassium) [20,29,31]. In general, this type of base oils has the following advantages: wide range of viscosity, low pour points, good thermal stability, high flash points, good lubricity, low toxicity, good shear stability, non-corrosive and its decomposition into volatile products, among others. However, it is important to mention its poor compatibility with mineral and PAO oils [32]. They are still relatively expensive products, but they present a wide variety of applications: industrial gear greases and oils, compressor lubricants, metallurgical fluids, hydraulic fluids resistant to fire and cooling.

Finally, the third category in the classification of the base lubricants is the bio-based oils, which may be of vegetable or animal origin. In the last decades, interest on these fluids has grown because of the hardening of the government regulations related to environmental issues [33]. From the CEC-L 33-T 82 biodegradability test, if 90% or more of a sample is degraded, the lubricant is considered highly biodegradable. Usually, mineral oils and PAOs degrade 20 to 40%, however trimellitates, polyolesters and polyalkylene glycols more than 90% [29]. Vegetable oils reveal some improvement over mineral and synthetic bases such as, their high biodegradability, low toxicity and bioaccumulation, also to the fact that they come from renewable sources and represent a great alternative to fossil carbon-based fuels [34]. Added to this, vegetable oils have other advantages, such as high flash point, very low volatility, good viscosity/temperature relationship, and high lubricity. These oils present a main disadvantage for their use as lubricants, since they possess poor thermal and oxidative stabilities [35]. Among its multiple applications we should remark their use as comprise engine oils, transmission oils and hydraulic fluids [20,36].

As has been remarked above, a fully-formulated lubricant contains usually around 93 % of base oils and 7 % of chemical additives [37,38]. Additives are organic or inorganic compounds dissolved or suspended in the base oil. The additive effects on base oil behaviour could be improve some already existing property, suppress undesirable changes that can appear during the service life or give a new quality [39]. It is crucial the correct selection of lubricant additives according to the final application. It is possible to classify the additives according to which part of the tribological system they affect [40,41]. Table 1.1 shows a schematic classification of several type of additives and the property each one can modify. Additives technology needs to be developed to improve the properties and performance of

advanced lubricants and to cover the demand of market for automotive oils, industrial oils, and metalworking fluids that is growing rapidly.

Table 1.1. Lubricant additives classification [40].

Modifiers (base oil properties)	**Property**
Viscosity improvers	Pressure-viscosity coefficient, viscosity index, film-thickness
Pour-point depressants	VT behaviour
Demulsifiers/Emulsifiers	Phase separation
Flow improvers	Rheological behaviour
Antioxidants	Thermal degradation
Modifiers (metal surface properties)	**Property**
Friction modifiers	Friction coefficient
Anti-wear additives	Wear
Corrosion additives	Corrosion inhibition
Extreme pressure additives	Scratch resistance

Friction modifiers (FMs) are applied mainly on boundary and mixed lubrication regimes [42]. In addition to help to reduce friction losses, this type of additives can achieve to improve load-carrying capability and decrease the emissions and fuel consumption [3]. Recently, Spikes [43] has published a review on friction modifier additives usually employed in lubrication. Spikes focuses its attention on: organic friction modifiers, functionalized polymers, soluble organo-molybdenum additives and dispersed nanoparticles. The interest in using colloidal solid particles in the size range 1 to 500 nm as friction and wear reduction additives has been increasing in the last years. The main reason to use nanoparticles as lubricant additives is due to their reduced size, which allows nanoparticles access to remote areas (defects) of the contact surfaces, producing subsequently an advisable lubrication effect [44].

1.3. Nanoparticles as Additives

Currently, nanotechnology has become an interesting field for lubrication, owing to this, a huge number of researchers [45-55] have explore the idea to use nanoparticles as anti-friction and anti-wear additives. Some potential advantages of using nanoparticles as lubricant additives have been reported by Spikes [43]. Mainly, they can be summarized in: low interaction with other additives; ability to form film on different surface types; they are more durable and inert with other additives; highly non-volatile and adequate to tolerate high temperatures. As shows Table 1.2, nanoparticles used as friction modifiers additives can

perform four different lubrication mechanisms: rolling effect, tribo-film, mending effect and polishing. The rolling effect and tribo-film mechanisms are related with the presence of the nanoparticles however mending and polishing effects are due to the interaction between the surface and the nanoparticles [42].

Table 1.2. Main lubrication mechanisms of nanoparticles as additives [12,56].

Mechanism	Description	Schematic Graphical
Rolling	Spherical nanoparticles are prone to roll between the two sliding surfaces.	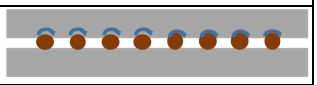
Tribo-film	Nanoparticles form a protective film that protects the surrounding surfaces.	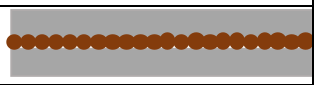
Mending	Nanoparticles tend to fill the microcracks and repair microdamages on rubbing surface.	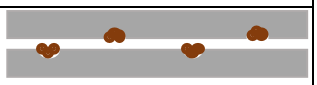
Polishing	Hard nanoparticles provide a mechanical polishing of rubbing surfaces.	

Nanoparticles (NPs) can be classified in different types according to their size, morphology, physical and chemical properties [57]. An interesting classification was recently proposed by Dai *et al*. [56] according to their chemical structure. Thus, NPs were divided into seven types: carbon-based nanoparticles and its derivatives, metals, metal oxide, sulfides, rare earth compounds, nanocomposites and others. The carbon-based nanomaterials includes carbon nano-onions, carbon nanotubes, carbon nanohorns, fullerenes, nanodiamonds, graphenes, and nanoPTFEs [58]. These nanomaterials are composed essentially of carbon and can present diverse morphologies, such as spherical or ellipsoidal (corresponding to fullerenes) or cylindrical (typically referred as nanotubes). Fullerenes are a carbon allotrope, their hollow spherical structure is composed of closed carbon cages formed by pentagons and hexagons. Their main properties include: electrical conductivity, high strength, electronic affinity and versatility [59]. Carbon nanotubes (CNTs) have tubular structure with diameter 1–2 nm, while their length can be of several micrometers [60]. They are as a sheet of graphite rolled up into a cylinder, according to the number of carbon layer, they can be named as single-walled (SWNTs) or multi-walled carbon nanotubes (MWNTs) [61]. These nanoadditives can be used in multiple applications, especially to enhance films and coatings in lubrication systems [62,63]. Carbon materials have much interest in the tribology field due to their high chemical stability and excellent mechanical, thermal, chemical and electrical properties [42,64]. It is interesting to note that the two-dimensional structure of graphene exhibits a higher lubrication potential than other nanostructured carbon allotropes, such as one-dimensional nanotubes or zero-dimensional fullerenes [65]. Kiu *et*

al. [66] have evaluated the tribological properties of graphene nanoparticles as lubricant additive in a vegetable oil. They concluded that graphene nanoadditives reduce both the friction coefficient and the wear scar diameter. Varrla *et al*. [67] have also investigated the tribological behaviour of a graphene based engine oil nanodispersions, finding a great performance on the tribological properties. These authors attribute this fact to the extreme mechanical strength and nanobearing lubrication mechanism of graphene. Nunn *et al*. [68] have studied the tribological properties of an polyalphaolefin (PAO) modified with nanocarbon additives. In addition, the performance of nanocarbon particles in PAO in combination with molybdenum dialkyldithiophosphate was also investigated. These authors observed a significant increase in the wear as compared to pure PAO when nanodiamonds particles (NDs) and onion-like carbon (OLDs) were additivated.

Metal nanoparticles have excellent chemical and physical properties, such as unique thermal, electronic, magnetic, optical, chemical and catalytic characteristics [69]. There are many research in which several metallic nanoparticles have been applied as lubricant additives, including Cu, Fe, Co, Ag, Pd, Ni or Au [56]. The use of these nanoparticles additives in lubricating oils provides good friction reduction and anti-wear behavior [46,70,71]. Padgurskas *et al*. [46] have performed tribological test with Fe, Cu and Co nanoparticles added to mineral oil. All nanoparticles have provided a significant decrease of friction and wear properties, being Cu nanoparticles those for which Padgurskas *et al*. have obtained the best results. Qiu *et al*. [71] have evaluated the tribological behavior of Ni nanoparticles as additives in lubricating oils. They have concluded that Ni nanoparticles improve the friction and wear properties of lubricants due to the formation of a deposit film in the contacting regions. Maliar *et al*. [72] have studied the lubricated friction and wear behaviour of the rapeseed and mineral oils with and without surfactant/iron particles. These authors have remarked that the addition of 0.1 wt% of Fe nanoparticles in rapeseed oil produces an increase of the friction coefficient but a reduction of the wear.

Metal oxide nanoparticles can be composed of a variety of diverse materials, including zirconium, titanium, zinc, copper, cerium, aluminium and iron oxides. Hernández Battez *et al*. [73] have discussed the tribological behaviour of CuO, ZrO_2 and ZnO nanoparticles as antiwear additives of a polyalphaolefin (PAO6). These authors conclude that all nanoparticle dispersions can reduce the friction coefficient and increase anti-wear ability of base oil (PAO6). Patil *et al*. [54] have published a review about tribological properties of several metal oxide nanoparticles, such as CuO, TiO_2 and CeO_2 as anti-friction and anti-wear additives. Wu *et al*. [48] have examined the tribological behavior of two

different lubricants, an engine oil and a base oil, additivated with CuO, TiO_2, and nanodiamond nanoparticles. The results obtained by these authors have shown that all nanoadditives exhibit excellent friction reduction and anti-wear behavior, in particular CuO nanoparticles. Ingole *et al*. [74] have investigated the effects of titanium dioxide nanoparticles on the tribological behavior of a mineral oil. An increment of the friction coefficient in comparison with the base oil for all the compositions was observed when commercially available TiO_2 nanoparticles were used.

Sulfides nanomaterials (usually molybdenum disulfide, MoS_2 and tungsten disulfide, WS_2) have been used as friction modifier additives due to their layered structure. From these inorganic additives, which have a laminar structure, inorganic fullerene-like (IF) nanoparticles are obtained [75]. Molybdenum disulfide is mainly employed with greases because of its insolubility in hydrocarbon media. Their synthesis is quite difficult and involves toxic reactants [76]. Sgroi *et al*. [77] have employed MoS_2 nanoparticles as lubricant additive for an engine oil, modifying the original additive package of the lubricant in order to obtain a stable dispersion. Tribological tests demonstrated a significant improvement of friction-reduction in all lubrication regimes and of anti-wear properties of the formulated nanolubricant in comparison with the standard additive package. Shi *et al*. [78] have tested the tribological behaviour of a motor oil additivated with WS_2 nanoparticles. They have also observed that the additivation of the motor oil with tungsten disulfide shows better lubrication properties than the original motor oil. Sulfides show excellent friction reduction and anti-wear abilities, however their high content of sulfur is a huge disadvantage in respect of the environmental sustainability [56].

Rare earth compounds have been widely investigated. Their hexagonal crystal layer structure implies good friction-reducing and anti-wear behavior [79]. Rare-earth compounds can reduce the lubrication consumption and improve the anti-wear capacity of machine [80]. Certain rare earth compounds, specially, La and Ce elements, are doped with nanoparticles as TiO_2 [56]. For instance, Gu *et al*. [81] have examined the tribological properties of oleic acid surface-capped lanthanum-doped titanium dioxide composite nanoparticles (OA/La-TiO_2) in rapeseed oil. The results suggested that OA/La-TiO_2 nanoparticles used as additives were able to improve anti-wear and friction-reducing capabilities of base oil.

Nanocomposites are materials in which at least one of the phases shows dimensions in the nanometre range [82]. The nanocomposites may be prepared by mechanical mixing, chemical synthesis and coating technology. Current researches [83-86] have reported that with nanocomposites better tribological performances can be achieved in comparisons with

original nanoparticles. Nanocomposites include Cu/SiO_2, Al_2O_3/SiO_2, Al_2O_3/TiO_2, Cu/GO, (rGO)/ZrO_2, among others [56]. Luo *et al*. [87] have studied the tribology properties of Al_2O_3/TiO_2 nanocomposites concluding that reduce significantly friction coefficient and improve anti-wear performance. Furthermore, Al_2O_3/TiO_2 nanoparticles exhibit better anti-wear and anti-friction effect than the pure compounds separately. Zhou *et al*. [88] have also examined the tribological behaviour of a paraffinic oil additivated with a nanocomposite of zirconia (ZrO_2) nanoparticles and reduced graphene oxide (rGO) nanosheets. The results obtained by Zhou *et al*. shown outstanding friction-reduction and anti-wear properties associated with the nanocomposite. Moreover, they observed a high load-bearing capacity due to the synergetic effect between rGO nanosheets and ZrO_2 nanoparticles.

The classification proposed by Dai *et al*. [39] also include other nanoadditives such as: BN, $CaCO_3$, $ZnAl_2O_4$, Zeolite, ZrP, SiO_2, PTFE, hydroxide, among others. Baş and Karabacak [89] have investigated the effect of boron compounds (hexagonal boron nitride, hBN and boric acid, BA) on lubrication oils. They have concluded that boron compound additives reduce the friction coefficient in engine oils forming a tribofilm in boundary or mixed lubrication regimes. Wan *et al*. [90] have also studied the tribological properties of a commercial lubricant oil containing boron nitride (BN) nanoparticles. Li *et al*. [91] have studied tribological behavior of SiO_2 nanoparticles as additives. They demonstrated that nano-silica exhibit friction and wear reduction compared to the neat lubricant.

For the application of nanoparticles as lubricant additives it is necessary not only to analyse the tribological behaviour of the nanolubricants, but also to rigorously study their thermophysical (viscosity, density, thermal conductivity and compressibility) and rheological properties (flow curves). The thermophysical properties of nanolubricants are very important for heat transfer performance of machines, for that reason these properties should be discussed. The thermophysical behaviour depends on several factors such as the base oil used for the formulation of the nanolubricant, the nanoparticles size, shape and concentration, together with the temperature and pressure operating of the machinery for which the nanolubricant is developed. Concerning thermophysical properties several studies have been published in the last decade. Thus, Jatti *et al*. [92] have studied the effect of CuO nanoparticle on viscosity of mineral oil. They observed that there is no noticeable change in viscosity at lower nanoparticle concentrations. Kotia *et al*. [93] have also researched the influence of CuO nanoparticles on thermophysical properties of a hydraulic oil showing a low variation in viscosity of prepared nanolubricants. Kole and Dey [94] have also employed CuO nanoparticles as nanoadditives in a gear oil. They have observed an increase of the

viscosity with the volume fraction of nanoparticles. Kedzierski *et al*. [95] have investigated the effect on several thermophysical properties (kinematic viscosity, density, and thermal conductivity) of a nanolubricant based on a synthetic polyolester, aluminum oxide (Al_2O_3) and zinc oxide (ZnO) nanoparticles. An increment in all these properties with the nanoparticle mass fraction was observed. Ali *et al*. [96] have checked the influence on the thermal conductivity and the viscosity of Al_2O_3, TiO_2 and Al_2O_3/TiO_2 hybrid nanoparticles suspended in 5W-30 engine oil. All the nanolubricants showed a remarkable increase in thermal conductivity, in particular Al_2O_3/TiO_2 hybrid-based nanodispersions. The addition of nanoadditives slightly decrease the kinematic viscosity. Su *et al*. [97] have also analysed the thermal conductivity and the viscosity of graphite oil-based nanolubricants, using as base oils a vegetable oil and an unsaturated polyol ester. The addition of graphite nanoparticles increased the viscosity and thermal conductivity of both base oils. Recently, Kotia *et al*. [98] have published a review about the thermophysical and tribological properties of nanolubricants. These authors outline that the viscosity and density increase with the nanoparticles volume fraction, specifically when smaller size and higher volume fraction were used. Kotia *et al*. remark that friction properties of nanolubricant, such as friction coefficient and wear, are significantly enhanced due to the lubrication mechanisms of nanoadditives (Table 1.2).

On the other hand, other important challenge for the preparation and future implementation in the industry of the nanolubricants is to be able to ensure a homogenous and stable nanodispersion. Prior to the tribological and the thermophysical studies of the nanolubricants, relevant knowledge about their dispersion stability is required, since this point is crucial in their industrial implementation [97]. However, there are scarce articles analyzing the stability of the nanolubricants. The major part of the publications are focused on thermal nanofluids and not in nanolubricants. Shahnazar *et al*. [15] have recently published a review about the improvement that nanoadditives produce on the performance of traditional solid lubricant additives, but also reflect the trouble to prepare and maintain homogenous nanolubricant dispersions. In addition to the thermophysical analysis, Su *et al*. [97] have studied the dispersion stability of graphite in vegetable oil and in an unsaturated polyol ester at different ultrasonication times using a zeta potential analysis. The unsaturated polyol ester-based nanodispersions showed much better stability results, due to their higher viscosity. Kole and Dey [94] have analyzed the stability of CuO-gear oil based nanodispersions using oleic acid as surfactant. These authors remarks that any visual nanoparticle sedimentation was shown for more than thirty days. Rashin and Hemalatha [99]

have studied the dispersion stability of ZnO-coconut oil nanodispersions using visual control and UV–visible optical transmittance method. They start to observe sedimentation seven days after the nanodispersion preparation. Song *et al*. [100] have compared the dispersibility of $ZnAl_2O_4$ modified at different temperatures and several modifier concentration. These authors concluded that the nanoadditive concentration and heating temperature are both important aspects for improving the temporal stability of nanolubricants. A large amount of works on the tribological behavior of nanolubricants does not report on the temporal stability or not include empirical proof of long-term stability of nanolubricants [13].

1.4. Framework of this PhD Thesis

This PhD Thesis was carried out in the Laboratory of Thermophysical Properties and the Laboratory of Thermophysical and Surface Properties of Liquids of the Applied Physics Department of the University of Santiago de Compostela. The Laboratory of Thermophysical Properties belongs to the research group NaFoMat "Nanomaterials, Photonics and Soft Matter" (GI-1488). This research group has obtained funding from the Consellería de Cultura, Educación e Ordenación Universitaria (Xunta de Galicia) as competitive reference group (GRC ED431C 2016/001). This program offers funding to the research groups characterized by their high scientific production and their I+D performance. Moreover, NaFoMat group is part of the Materials Strategic Agrupation-AEMAT (AGRUP2015/11) of the University of Santiago de Compostela.

This PhD Thesis was carried out in the background of two larger national research projects. The first project titled “Development of thermal fluids and lubricants based on nanoaditives for the production, storage use of energy efficient”, (NanoLuter, ENE2014-55489-C2-1-R) was supported by Spanish Ministry of Economy and Competitiveness and the UE FEDER programme. This project was coordinated with the University of Vigo. The aims of this project were to develop nanolubricants for several applications in renewable energy and automotive systems and to study their stability and thermophysical, rheological and tribological behaviour. The second national project titled “Development of hybrid nanofluids, nanolubricants and nano-enhanced Phase Change Materials for the transfer, storage and production of energy”, (AdLuter, ENE2017-86425-C2-2-R) was supported by Spanish Ministry of Economy and Competitiveness. This project was also coordinated with the University of Vigo. Its objective is to propose new advanced materials specialized in the field of lubrication, storage and transfer of thermal energy mainly focused in the field

of renewable energies (solar, wind, hydraulic and geothermal) and in engines and automotive transmissions.

Furthermore, a part of this PhD Thesis was realized during a stay of three months in the Instituto de Ciência e Inovação em Engenharia Mecânica e Engenharia Industrial (INEGI) of the Faculdade de Engenharia da Universidade do Porto (FEUP) under the supervision of Prof. Seabra. This stay was funded by the IACOBUS Program 2017. The main objective of this program is to promote cooperation between the human resources of the higher education institutions of the Euro region Galicia - North of Portugal. This initiative is pioneer in Europe and its managing entity is the Agrupación Europea de Cooperación Territorial Galicia–Norte de Portugal (GNP, AECT).

1.5. Objectives

This work is focused on the study of both neat lubricants and new nanolubricant formulations. Tables 1.3 and 1.4 report the main characteristics of the base oils and the nanoparticles studied. This PhD Thesis is the first one realized in our research group on this matter. It has been divided into three areas of study: lubricant formulation by using nanoparticles as additives, thermophysical properties characterization and determination of the tribological behaviour. The main objectives of this PhD Thesis can be summarized as:

-Formulation of new lubricants based on synthetic oils and nanoparticles of different morphology (spherical, rod-like and laminar): installation and start-up of specific technical apparatus.

-Study of the scientific techniques suitable for the control of the nanolubricant temporal stability, sedimentation rate and aggregation level.

-Characterization of nanolubricants with different chemical structures: viscosity index, density, dynamic viscosity, speed of sound, flow properties and thermal conductivity.

-Determination of the volumetric and viscous behavior of several base oils at high pressures: reliable equation of state and viscosity pressure-coefficient for elastohydrodynamic lubrication.

-Measure of the film thickness, friction properties and wear of pure base oils and nanolubricants: effect of the entrainment speed, slide-to-roll ratio and roughness.

-Analysis of the influence of the morphology, concentration and size of the nanoparticles on the thermophysical and tribological properties of the nanolubricants.

Table 1.3. Properties of base lubricants studied in this PhD Thesis: *v*, kinematic viscosity and VI, viscosity index.

Lubricants				
Reduced Name	Source	v^a (313.15 K) / cSt	VI	Chemical structure
Gr I base oil / SN 230	Repsol	48.2	98	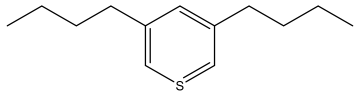
Gr III base oil	Repsol	36.5	129	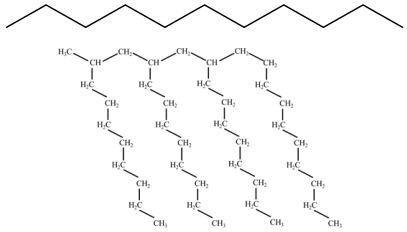
Gr IV base oil / PAO6	Repsol	29.8	137	
Gr V base oil / TMP+NPG	Repsol	38.5	191	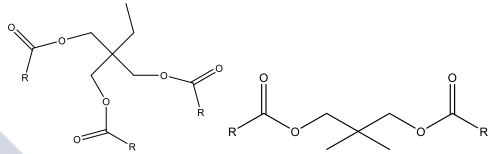
75W40 Formulated oil	Repsol	65.6	228	-
15W40 Formulated oil	Repsol	104	138	-
PAG2	Croda	60.0	220 [101]	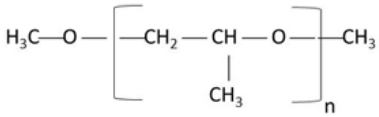
TTM	Verkol Lubricantes	319.0	74 [102]	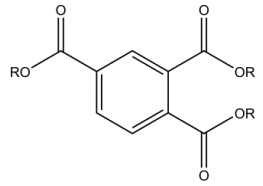

[a] Determined in this work by using Anton Paar Stabinger SVM3000 apparatus.

Table 1.3. ***(Continued)*** Properties of base lubricants studied in this PhD Thesis: v, kinematic viscosity and VI, viscosity index.

Lubricants				
Reduced Name	Source	v^a (313.15 K) / cSt	VI	Chemical structure
BIOE	Verkol Lubricantes	497.0	155 [102]	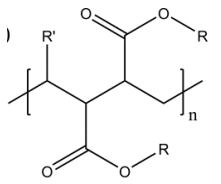
TMPTO	Croda	49.0	190	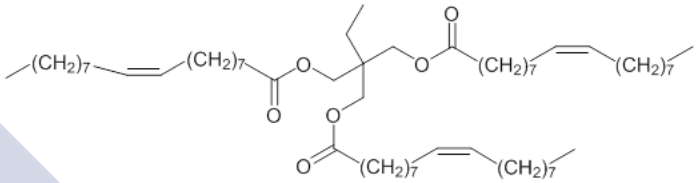

[a] Determined in this work by using Anton Paar Stabinger SVM3000 apparatus.

Table 1.4. Characteristics of the nanoadditives used in this PhD Thesis.

Nanoadditives				
Chemical Name	Source	Mole Fraction Purity[a]	Analysis Method	Average size / nm
ZrO_2 nanoparticles	Iolitec	0.999	ICP-AES	30-60
BN nanoparticles	Iolitec	0.99	XRF	70
Graphene nanoplatelets	Iolitec	0.995	Loss of Ignition and Raman	11-15[b]

[a] Determined by the supplier.
[b] Referred to thickness

1.6. References

[1] K. Holmberg, A. Erdemir, Influence of tribology on global energy consumption, costs and emissions, Friction 5 (2017) 263-284.
[2] B. Gupta, N. Kumar, K. Panda, S. Dash, A.K. Tyagi, Energy efficient reduced graphene oxide additives: Mechanism of effective lubrication and antiwear properties, Sci. Rep. 6 (2016) 18372.
[3] D. Kenbeck, T.F. Bunemann, Organic friction modifiers. in: L.R. Rudnick (Ed.), Lubricant Additives: Chemistry and Applications, 3rd Edition, CRC Press, Boca Raton, 2017.
[4] I. Tzanakis, M. Hadfield, B. Thomas, S.M. Noya, I. Henshaw, S. Austen, Future perspectives on sustainable tribology, Renew. Sustain. Energy Rev. 16 (2012) 4126-4140.
[5] G. Paul, H. Hirani, T. Kuila, N. Murmu, Nanolubricants Dispersed with Graphene and its Derivatives: An Assessment and Review of the Tribological Performance, Nanoscale 11 (2019) 3458-3483.
[6] N.S. Ahmed, A.M. Nassar, Lubrication and Lubricants, in: J. Gegner (Ed.), Tribology-Fundamentals and Advancements, InTechOpen, 2013, pp. 55-76.
[7] Y. Zhang, Boundary lubrication—An important lubrication in the following time, J. Mol. Liq. 128 (2006) 56-59.
[8] M.C. Kocsis, P. Morgan, A. Michlberger, E.E. Delbridge, O. Smith, Optimizing Engine Oils for Fuel Economy with Advanced Test Methods, SAE Int. J. Fuels Lubr. 10 (2017).
[9] A. Kotia, G.K. Ghosh, I. Srivastava, P. Deval, S.K. Ghosh, Mechanism for improvement of friction/wear by using Al_2O_3 and SiO_2/Gear oil nanolubricants, J. Alloys Compd. 782 (2019) 592-599.
[10] M.J. Plumley, V.W. Wong, T.V. Martins, Demonstrating Improved Fuel Economy Using Subsystem Specific Lubricants on a Modified Diesel Engine, Tribol. Trans. 60 (2017) 490-496.
[11] B.J. Hamrock, S.R. Schmid, B.O. Jacobson, Fundamentals of Fluid Film Lubrication, 2nd Edition, CRC Press, 2004.
[12] L. Kong, J. Sun, Y. Bao, Preparation, characterization and tribological mechanism of nanofluids, RSC Advances 7 (2017) 12599-12609.
[13] Y. Chen, P. Renner, H. Liang, Dispersion of Nanoparticles in Lubricating Oil: A Critical Review, Lubricants 7 (2019) 7.
[14] M. Gulzar, H.H. Masjuki, M.A. Kalam, M. Varman, N.W. Mohd Zulkifli, R. Mufti, R. Zahid, Tribological performance of nanoparticles as lubricating oil additives, J. Nanopart. Res. 18 (2016) 223.
[15] S. Shahnazar, S. Bagheri, S.B. Abd Hamid, Enhancing lubricant properties by nanoparticle additives, Int. J. Hyd. Energy 41 (2016) 3153-3170.
[16] R. Stribeck, Kugellager für beliebige Belastungen, Springer, 1901.
[17] R. Stribeck, Die wesentlichen Eigenschaften der Gleit- und Rollenlager, Springer, 1903.
[18] S. Loehle, Understanding of adsorption mechanism and tribological behaviors of C_{18} fatty acids on iron-based surfaces: a molecular simulation approach, (PhD Thesis), Ecole Centrale de Lyon, 2014.
[19] M.M. Khonsari, E.R. Booser, Applied Tribology: Bearing Design and Lubrication, 2nd Edition, John Wiley & Sons, 2008.
[20] L.R. Rudnick, S.Z. Erhan, Synthetic, Mineral Oils and Bio-based Lubricants, 2nd Edition. CRC Press Taylor and Francis Group, London, 2013.
[21] A.R. Lansdown, Lubrication and Lubricant Selection: A Practical Guide, 3rd Edition, John Wiley & Sons, 2004.

[22] Y. Bertrand, L.C. Hoang, Vegetal oils as substitute for mineral oils. Proceedings of the 7th International Conference on Properties and Applications of Dielectric Materials, Japan, 2003.
[23] L.R. Rudnick, W.J. Bartz, Comparison of Synthetic, Mineral Oil, and Bio-Based Lubricant Fluids. in: L.R. Rudnick, (Ed.), Synthetic, Mineral Oils and Bio-based Lubricants, CRC Press Taylor and Francis Group, Boca Raton, London, 2013.
[24] W. Dresel, Synthetic Base Oils. in: W. Dresel, T. Mang, (Eds.), Lubricants and Lubrication, Wiley-VCH Verlag GmbH & Co. KGaA, Weinheim, 2017, pp. 83-115.
[25] A. Voelkel, J. Fall, Chromatographic and non-chromatographic characterization of poly-α-olefins, J. Synth. Lubr. 24 (2007) 91-100.
[26] R. Benda, J. Bullen, A. Plomer, Synthetics basics: Polyalphaolefins - base fluids for high-performance lubricants, J. Synth. Lubr. 13 (1996) 41-57.
[27] S.J. Randles, Esters. in: L.R. Rudnick, (Ed.), Synthetic, Mineral Oils and Bio-based Lubricants, CRC Press Taylor and Francis Group, Boca Raton, London, 2013.
[28] Wiley, Ullmann's Polymers and Plastics: Products and Processes, 4 Volume, W. Wiley-VCH, 2016.
[29] R. Booser, CRC Handbook of Lubrication and Tribology Volume III Monitoring, Materials, Synthetic Lubricants, and Applications, CRC Press, Inc., Boca Raton, 1994.
[30] Polyalkylene Glycol Synthetic PAGs Explained.
https://www.machinerylubrication.com/Read/930/pag-synthetic-oil, 2006.
[31] P.L. Matlock, W.L. Brown, N.A. Clinton, Polyalkylene glycols. in: L.R. Rudnick, R.L. Shubkin, (Eds.), Synthetic lubricants and high-performance functional fluids, Marcel Dekker, Inc. New York, 1999.
[32] M. Brown, J.D. Fotheringham, T.J. Hoyes, R.M. Mortier, S.T. Orszulik, S.J. Randles, P.M. Stroud, Synthetic base fluids. in: R.M. Mortier, M.F. Fox, S.T. Orszulik, (Eds.), Chemistry and Technology of Lubricants, Springer, London, 2010, pp. 35-74.
[33] L.R. Rudnick, S.Z. Erhan, Natural Oils as Lubricants in: L.R. Rudnick, (Ed.), Synthetic, Mineral Oils and Bio-based Lubricants, CRC Press Taylor and Francis Group, Boca Raton, London, 2013.
[34] R. Garcés, E. Martínez-Force, J.J. Salas, Vegetable oil basestocks for lubricants, Grasas y aceites 62 (2011) 8.
[35] L.A. Quinchia, M.A. Delgado, C. Valencia, J.M. Franco, C. Gallegos, Natural and Synthetic Antioxidant Additives for Improving the Performance of New Biolubricant Formulations, J. Agric. Food Chem. 59 (2011) 12917-12924.
[36] I. Gawrilow, Vegetable oil usage in lubricants, Inform., 15 (2004) 702–705.
[37] J.C.J. Bart, E. Gucciardi, S. Cavallaro, 7 - Formulating lubricating oils. in: J.C.J. Bart, E. Gucciardi, S. Cavallaro, (Eds.), Biolubricants, Woodhead Publishing, 2013, pp. 351-395.
[38] T. Mang, Lubricants and their Market. in: W. Dresel, T. Mang, (Eds.), Lubricants and Lubrication, Wiley-VCH Verlag GmbH & Co. KGaA, Weinheim, 2017.
[39] Lubricant Additives - A Practical Guide.
https://www.machinerylubrication.com/Read/31107/oil-lubricant-additives.
[40] J. Braun, Additives, Lubricants and lubrication, Wiley-VCH Verlag GmbH & Co. KGaA, Weinheim, 2007, pp. 88-118.
[41] L.R. Rudnick, Lubricant Additives: Chemistry and Applications, 3rd Edition, CRC Press Taylor and Francis Group, Boca Raton, 2017.
[42] Z. Tang, S. Li, A review of recent developments of friction modifiers for liquid lubricants (2007–present), Curr. Opin. Solid State Mater. Sci. 18 (2014) 119-139.
[43] H. Spikes, Friction Modifier Additives, Tribol. Lett. 60 (2015) 1-26.

[44] N.G. Demas, E.V. Timofeeva, J.L. Routbort, G.R. Fenske, Tribological Effects of BN and MoS_2 Nanoparticles Added to Polyalphaolefin Oil in Piston Skirt/Cylinder Liner Tests, Tribol. Lett. 47 (2012) 91-102.
[45] Z.S. Hu, R. Lai, F. Lou, L.G. Wang, Z.L. Chen, G.X. Chen, J.X. Dong, Preparation and tribological properties of nanometer magnesium borate as lubricating oil additive, Wear 252 (2002) 370-374.
[46] J. Padgurskas, R. Rukuiza, I. Prosyčevas, R. Kreivaitis, Tribological properties of lubricant additives of Fe, Cu and Co nanoparticles, Tribol. Int. 60 (2013) 224-232.
[47] M.V. Thottackkad, R.K. Perikinalil, P.N. Kumarapillai, Experimental evaluation on the tribological properties of coconut oil by the addition of CuO nanoparticles, Int. J. Precis. Eng. Manuf. 13 (2012) 111-116.
[48] Y.Y. Wu, W.C. Tsui, T.C. Liu, Experimental analysis of tribological properties of lubricating oils with nanoparticle additives, Wear 262 (2007) 819-825.
[49] B. Bhushan, Nanotribology and Nanomechanics: An Introduction, Springer, Berlin, Heidelberg, 2008.
[50] F. Dassenoy, L. Joly-Pottuz, J.M. Martin, D. Vrbanic, A. Mrzel, D. Mihailovic, W. Vogel, G. Montagnac, Tribological performances of $Mo_6S_3I_6$ nanowires, J. Eur. Ceram. Soc. 27 (2007) 915-919.
[51] P. Du, G. Chen, S. Song, H. Chen, J. Li, Y. Shao, Tribological Properties of Muscovite, CeO_2 and Their Composite Particles as Lubricant Additives, Tribol. Lett. 62 (2016) 29.
[52] N.W.M. Zulkifli, M.A. Kalam, H.H. Masjuki, R. Yunus, Experimental Analysis of Tribological Properties of Biolubricant with Nanoparticle Additive, Procedia Eng. 68 (2013) 152-157.
[53] C.-x. Gu, G.-j. Zhu, L. Li, X.-y. Tian, G.-y. Zhu, Tribological effects of oxide based nanoparticles in lubricating oils, J. Mar. Sci. Appl. 8 (2009) 71-76.
[54] S.J. Patil, D.P. Patil, A.P. Shrotri, V.P. Patil, A review on effect of addition of nano particles on tribological properties of lubricants, Int. J. Mech. Eng. Tech. 5 (2014) 120-129.
[55] A. Gautam, S. Prateek, A review on graphite and hybrid nano-materials as lubricant additives, IOP Conf. Ser.: Mater. Sci. Eng. 149 (2016) 012201.
[56] W. Dai, B. Kheireddin, H. Gao, H. Liang, Roles of nanoparticles in oil lubrication, Tribol. Int. 102 (2016) 88-98.
[57] I. Khan, K. Saeed, I. Khan, Nanoparticles: Properties, applications and toxicities, Arab. J. Chem. Open Acces (2017).
[58] L.O. Farng, T.-C. Jao, Ashless Antiwear and Antiscuffing (Extreme Pressure) Additives. in: L.R. Rudnick, (Ed.), Lubricant Additives: Chemistry and Applications, 3rd Edition, CRC Press, Boca Raton, 2017.
[59] A. Astefanei, O. Núñez, M.T. Galceran, Characterisation and determination of fullerenes: A critical review, Analytica Chimica Acta 882 (2015) 1-21.
[60] C. Liu, H.-M. Cheng, Carbon nanotubes: controlled growth and application, Mater. Today 16 (2013) 19-28.
[61] P. Pandey, M. Dahiya, Carbon nanotubes: Types, methods of preparation and applications, Int. J. Pharm. Sci. Res., 1 (2016) 15-21.
[62] C.S. Chen, X.H. Chen, L.S. Xu, Z. Yang, W.H. Li, Modification of multi-walled carbon nanotubes with fatty acid and their tribological properties as lubricant additive, Carbon 43 (2005) 1660-1666.
[63] J.A.C. Cornelio, P.A. Cuervo, L.M. Hoyos-Palacio, J. Lara-Romero, A. Toro, Tribological properties of carbon nanotubes as lubricant additive in oil and water for a wheel–rail system, J. Mater. Res. Technol. 5 (2016) 68-76.

[64] O. Penkov, H.-J. Kim, H.-J. Kim, D.-E. Kim, Tribology of Graphene: A Review, Int. J. Precis. Eng. Manuf. 15 (2014) 577-585.
[65] G.-J. Lee, C.K. Rhee, Enhanced thermal conductivity of nanofluids containing graphene nanoplatelets prepared by ultrasound irradiation, J. Mater. Sci. 49 (2014) 1506-1511.
[66] S.S.K. Kiu, S. Yusup, C.V. Soon, T. Arpin, S. Samion, R.N.M. Kamil, Tribological investigation of graphene as lubricant additive in vegetable oil, J. Phys. Sci. 28 (2017) 257–267.
[67] E. Varrla, S. Venkataraman, R. Sundara, Graphene-Based Engine Oil Nanofluids for Tribological Applications, ACS Appl. Mater. Interfaces 3 (2011) 4221-4227.
[68] N. Nunn, Z. Mahbooba, M.G. Ivanov, D.M. Ivanov, D.W. Brenner, O. Shenderova, Tribological properties of polyalphaolefin oil modified with nanocarbon additives, Diam. Relat. Mater. 54 (2015) 97-102.
[69] G. Yang, Z. Zhang, S. Zhang, L. Yu, P. Zhang, Synthesis and characterization of highly stable dispersions of copper nanoparticles by a novel one-pot method, Mater. Res. Bull. 48 (2013) 1716-1719.
[70] J. Zhou, J. Yang, Z. Zhang, W. Liu, Q. Xue, Study on the structure and tribological properties of surface-modified Cu nanoparticles, Mater. Res. Bull. 34 (1999) 1361-1367.
[71] S. Qiu, Z. Zhou, J. Dong, G. Chen, Preparation of Ni Nanoparticles and Evaluation of Their Tribological Performance as Potential Additives in Oils, J. Tribol. 123 (1999) 441-443.
[72] T. Maliar, S. Achanta, H. Cesiulis, D. Drees, Tribological behaviour of mineral and rapeseed oils containing iron particles, Ind. Lubr. Tribol. 67 (2015) 308-314.
[73] A. Hernández Battez, R. González, J.L. Viesca, J.E. Fernández, J.M. Díaz Fernández, A. Machado, R. Chou, J. Riba, CuO, ZrO_2 and ZnO nanoparticles as antiwear additive in oil lubricants, Wear 265 (2008) 422-428.
[74] S. Ingole, A. Charanpahari, A. Kakade, S.S. Umare, D.V. Bhatt, J. Menghani, Tribological behavior of nano TiO_2 as an additive in base oil, Wear 301 (2013) 776-785.
[75] R. Tenne, Fullerene-like materials and nanotubes from inorganic compounds with a layered (2-D) structure, Colloids Surf. A 208 (2002) 83-92.
[76] O.P. Parenago, V.N. Bakunin, G.N. Kuz'mina, A.Y. Suslov, L.M. Vedeneeva, Molybdenum Sulfide Nanoparticles as New-Type Additives to Hydrocarbon Lubricants, Dokl. Chem. 383 (2002) 86-88.
[77] M. Sgroi, F. Gili, D. Mangherini, I. Lahouij, F. Dassenoy, I. Garcia, I. Odriozola, G. Kraft, Friction Reduction Benefits in Valve-Train System Using IF-MoS_2 Added Engine Oil, Tribol. Trans. 58 (2015) 207-214.
[78] C. Shi, D.-h. Mao, H. Feng, Preparation of tungsten disulfide motor oil and its tribological characteristics, J. Cent. South Univ. Technol. 14 (2007) 673-678.
[79] L. Yu, M. Nie, Y. Lian, The tribological behaviour and application of rare earth lubricants, Wear 197 (1996) 206-210.
[80] T. Liu, X. Hu, E. Hu, Y. Xu, Tribological Behaviour of Rare-Earth Lubricating Oils. in: J.P. Davim, (Ed.), Modern Mechanical Engineering: Research, Development and Education, Springer, Berlin Heidelberg, 2014.
[81] K. Gu, B. Chen, Y. Chen, Preparation and tribological properties of lanthanum-doped TiO_2 nanoparticles in rapeseed oil, J. Rare Earths 31 (2013) 589-594.
[82] P. Camargo, K.G. Satyanarayana, F. Wypych, Nanocomposites: Synthesis, Structure, Properties and New Application Opportunities, Mater. Res. 12 (2009).
[83] M. Farsadi, S. Bagheri, N.A. Ismail, Nanocomposite of functionalized graphene and molybdenum disulfide as friction modifier additive for lubricant, J. Mol. Liq. 244 (2017) 304-308.
[84] J.P. Davim, Tribology of Nanocomposites, Springer, Berlin Heidelberg, 2013.

[85] Y. Meng, F. Su, Y. Chen, Au/Graphene Oxide Nanocomposite Synthesized in Supercritical CO_2 Fluid as Energy Efficient Lubricant Additive, ACS Appl. Mater. Inter. 9 (2017) 39549-39559.
[86] H. Li, L. Chen, Y. Zhang, X. Ji, S. Chen, H. Song, C. Li, H. Tang, Synthesis of $MoSe_2$/Reduced graphene oxide composites with improved tribological properties for oil-based additives, Cryst. Res. Technol. 49 (2014) 204-211.
[87] T. Luo, X. Wei, H. Zhao, G. Cai, X. Zheng, Tribology properties of Al_2O_3/TiO_2 nanocomposites as lubricant additives, Ceram. Int. 40 (2014) 10103-10109.
[88] Q. Zhou, J. Huang, J. Wang, Z. Yang, S. Liu, Z. Wang, S. Yang, Preparation of a reduced graphene oxide/zirconia nanocomposite and its application as a novel lubricant oil additive, RSC Advances 5 (2015) 91802-91812.
[89] H. Baş, Y.E. Karabacak, Investigation of the Effects of Boron Additives on the Performance of Engine Oil, Tribol. Trans. 57 (2014) 740-748.
[90] Q. Wan, y. Jin, P. Sun, Y. Ding, Tribological Behaviour of a Lubricant Oil Containing Boron Nitride Nanoparticles, Procedia Eng. 102 (2015) 1038-1045.
[91] X. Li, Z. Cao, Z. Zhang, H. Dang, Surface-modification in situ of nano-SiO_2 and its structure and tribological properties, Appl. Surf. Sci. 252 (2006) 7856-7861.
[92] V.S. Jatti, T.P. Singh, Copper oxide nano-particles as friction-reduction and anti-wear additives in lubricating oil, J. Mech. Sci. Technol. 29 (2015) 793-798.
[93] A. Kotia, A. Haldar, R. Kumar, P. Deval, S.K. Ghosh, Effect of copper oxide nanoparticles on thermophysical properties of hydraulic oil-based nanolubricants, J. Braz. Soc. Mech. Sci. & Eng. 39 (2017) 259-266.
[94] M. Kole, T.K. Dey, Effect of aggregation on the viscosity of copper oxide–gear oil nanofluids, Int. J. Therm. Sci. 50 (2011) 1741-1747.
[95] M.A. Kedzierski, R. Brignoli, K.T. Quine, J.S. Brown, Viscosity, density, and thermal conductivity of aluminum oxide and zinc oxide nanolubricants, Int. J. Refrig. 74 (2017) 3-11.
[96] M.K. Ahmed Ali, H. Xianjun, R.F. Turkson, Z. Peng, X. Chen, Enhancing the thermophysical properties and tribological behaviour of engine oils using nano-lubricant additives, RSC Advances 6 (2016) 77913-77924.
[97] Y. Su, L. Gong, D. Chen, Dispersion stability and thermophysical properties of environmentally friendly graphite oil–based nanofluids used in machining, Adv. Mech. Eng. 8 (2016).
[98] A. Kotia, P. Rajkhowa, G.S. Rao, S.K. Ghosh, Thermophysical and tribological properties of nanolubricants: A review, Heat Mass Transfer 54 (2018) 3493–3508.
[99] M. Nabeel Rashin, J. Hemalatha, Synthesis and viscosity studies of novel ecofriendly ZnO–coconut oil nanofluid, Exp. Therm. Fluid Sci. 51 (2013) 312-318.
[100] X. Song, S. Zheng, J. Zhang, W. Li, Q. Chen, B. Cao, Synthesis of monodispersed $ZnAl_2O_4$ nanoparticles and their tribology properties as lubricant additives, Mater. Res. Bull. 47 (2012) 4305-4310.
[101] X. Paredes, A.S. Pensado, M.J.P. Comuñas, J. Fernández, How Pressure Affects the Dynamic Viscosities of Two Poly(propylene glycol) Dimethyl Ether Lubricants, J. Chem. Eng. Data 55 (2010) 4088-4094.
[102] I.O. Fernández, Thermophysical and tribological properties of ionic liquids as neat lubricants and as additives of biodegradable base oils for renewable energies, (PhD Thesis), Universidade de Santiago de Compostela, 2014.

2. MATERIALS AND METHODS

USC
UNIVERSIDADE
DE SANTIAGO
DE COMPOSTELA

2. MATERIALS AND METHODS

This chapter outlines the sample preparation methods and the experimental techniques used in this PhD Thesis. The set-up, the experimental conditions and the description of the different apparatus used to characterize the thermophysical and tribological properties of the pure base oils and nanolubricants are presented.

2.1. Materials Characterization

Base oils and nanoparticles

The base oils studied in this PhD Thesis are synthetic, eight of them are base oils and two of them formulated lubricants. As it was reported in Table 1.3, these oils have been provided by the partners (Croda, Verkol and Repsol) which support the two national research projects NanoLuter (ENE2014-55489-C2-1-R) and AdLuter (ENE2017-86425-C2-2-R). These projects are the background of this PhD Thesis. Four esters have been used: trimethylolpropane trioleate (TMPTO), isotridecyl trimellitate (TTM), a biodegradable polymeric ester (BIOE) and a mixture of two esters, trimethylolpropane and neopentylglycol. This last fluid is named in this work as (G-V) due to it is categorised in the group V of the classification proposed by the American Petroleum Institute (API). The other synthetic oils tabulated in Table 1.3 are: a polyalkylene glycol (PAG2), a polyalphaolefin oil (PAO6) classified in the group IV of the API (G-IV), a paraffinic oil (SN-230) classified in the group I (G-I) and a hydrocracking oil of the group III (G-III). Moreover, two formulated oil (commercial lubricants) were also studied, a synthetic gearbox oil (75W40) and a synthetic motor oil (15W40).

Nanoparticles of different morphology have been used as lubricant additives as was reported in Table 1.4. The SEM micrographs of nanoparticles used can be shown in Figure 2.1. As has been detailed in Chapter 1, accordingly with the classification proposed by Dai *et al*. [1], the nanoparticles we have used are categorized in: metal oxide, carbon-based and others nanoadditives types. Thus, we have utilized as additives: zirconium oxide (ZrO_2) nanoparticles, graphene nanoplatelets (GnP) and boron nitride (BN) nanoparticles. ZrO_2 has fraction purity of 0.999 (lot INO059008), a nominal diameter of (30–60) nm and a bulk density of 5.9 g cm^{-3}. Graphene nanoplatelets (GnP) have a mole fraction purity of 0.995 (lot NCP068011), a medium size of (11–15) nm and a bulk density of 2.25 g cm^{-3}. Finally, boron nitride (BN) nanoparticles present a mole fraction purity of 0.99 (lot MNC018001), a

nominal diameter of 70 nm and a bulk density of 2.29 g cm^{-3}. All these nanoadditives were supplied by Iolitec.

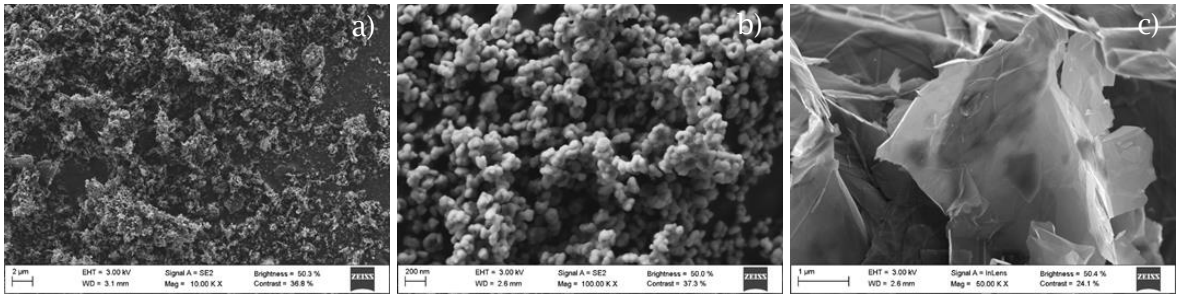

Figure 2.1. SEM micrographs of three different nanoparticles used in this PhD Thesis: boron nitride nanoparticles (a), spherically shaped ZrO_2 nanoparticles (b) and graphene nanoplatelets (c).

Characterization techniques

In this section the different techniques (mass spectrometry, nuclear magnetic resonance, scanning electron microscopy, transmission electron microscopy, Raman spectroscopy and X-ray diffraction) used to characterize both, the base oils and the nanoparticles, are briefly described. These experiments were realized in collaboration with the Research Support Services (RIAIDT) of the University of Santiago de Compostela.

Mass spectrometry: the base oils were analysed by mass spectrometry, with an Ultraflex III MALDI TOF (Bruker Daltonik GmbH, Bremen, Germany) apparatus equipped with a MALDI scoutMTPTM ionisation source and a "fast MCP-Gating" detection system. Figure 2.2 shows a picture of this apparatus. In addition, the weight-average molar mass, M_w, and the polydispersity index, Mw/Mn, was obtianed with the Polytool software (Bruker).

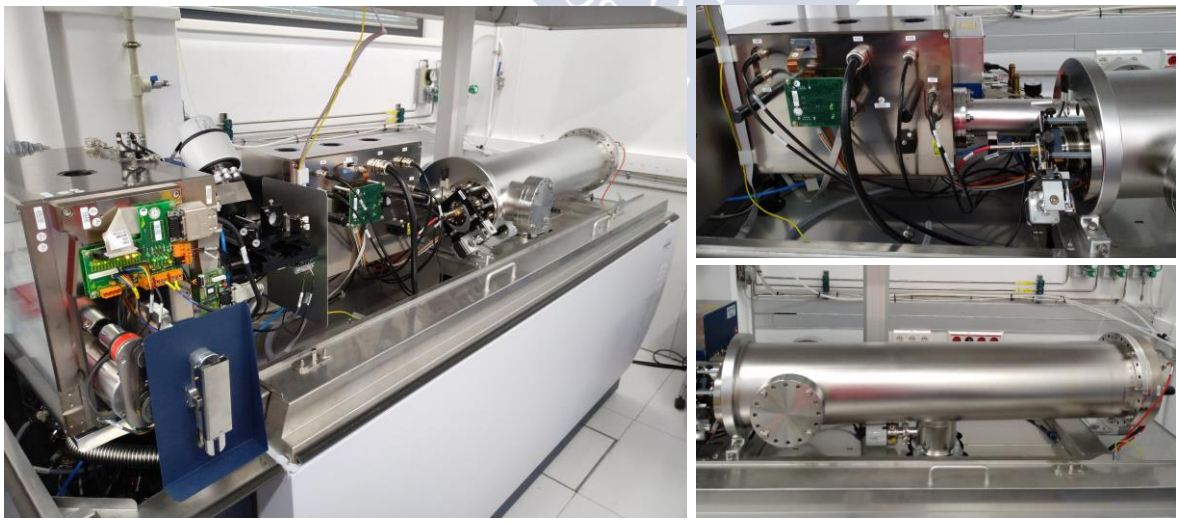

Figure 2.2. Maldi TOF/TOF mass spectrometer: image provided by Research Support Services (RIAIDT) of the University of Santiago de Compostela.

Nuclear Magnetic Resonance: mole fraction purity of some base oils used in this PhD Thesis was determined by Nuclear Magnetic Resonance (NMR) using a Bruker NEO 750 spectrometer (Figure 2.3). This apparatus operates at a frequency of 750 MHz (resonance ^{1}H) and allows to quantitatively determining the impurities present in the sample under study. This apparatus is equipped with three radiofrequency and deuterium channels, high power amplifiers and a PA-TXI-HFCN probe to NMR in solution (^{1}H-^{19}F/^{13}C/^{15}N).

Figure 2.3. Bruker NEO750 spectrometer. Images taken from http://www.usc.es/gl/investigacion/riaidt/index.html.

Scanning electron microscopy: the nanoparticles morphology was obtained by using a scanning electron microscope Zeiss FESEM Ultra Plus (SEM) (Figure 2.4) that operates at high vacuum mode. The nanopowder is placed on active carbon films supported by a carriage with multiple positions (Figure 2.4). The samples can also be analysed through a scanning transmission electron microscopy (STEM). Furthermore, Zeiss FESEM Ultra Plus is equipped with an additional detector for energy dispersive X-ray microanalysis (EDX). This detector (resolution 129ev and WD 8.5) can perform chemical elements distribution map and concentration profiles.

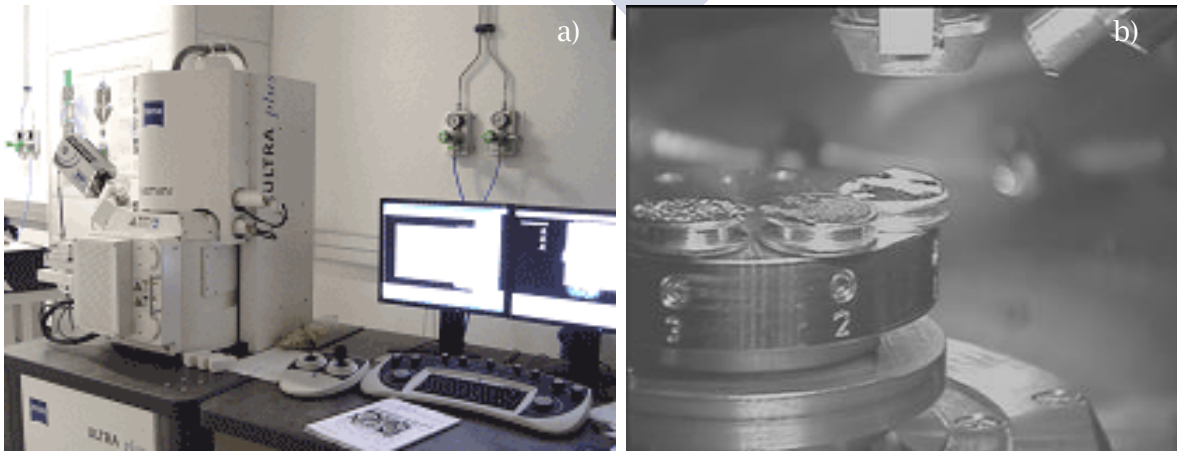

Figure 2.4. a) Zeiss FESEM Ultra Plus Scanning Electron Microscope and b) samples support. Images taken from http://www.usc.es/gl/investigacion/riaidt/index.html.

Transmission electron microscopy: a JEOL JEM-2010 high resolution transmission electron microscope (TEM) was used to analyse the size of the nanoparticles. For this task nanoadditives were dispersed in a solvent (1-buthanol). As we have observed high nanoparticles aggregation, it was not possible to obtain a nanoparticle size distribution. This technique cannot be used to control the aggregation in presence of the base oil due to it works under vacuum, so a highly volatile solvent should be used as base fluid. Figure 2.5 shows a photograph of this apparatus. It includes a high brightness lanthanum hexaboride (LaB6) filament. Moreover, it can operate at accelerating voltage from 80 to 200 kV. The grids used to support the samples are copper with a carbon film.

Figure 2.5. JEOL JEM-2010 Transmission Electron Microscope: image provided by Research Support Services (RIAIDT) of the University of Santiago de Compostela.

Raman spectroscopy: the number of graphene layers of graphene nanoplatelets was identified by Raman spectroscopy in the visible range, exactly at a wavelength of 514 nm. The Raman measurements were performed with a Renishaw confocal microscope model InVia Reflex using an argon ion laser. This apparatus (Figure 2.6) is equipped with a confocal LEICA DM microscope, a motorized platform XYZ for Raman mapping and a variable spot laser from 1 to 300 μm depending on the objective and the wavelength employed.

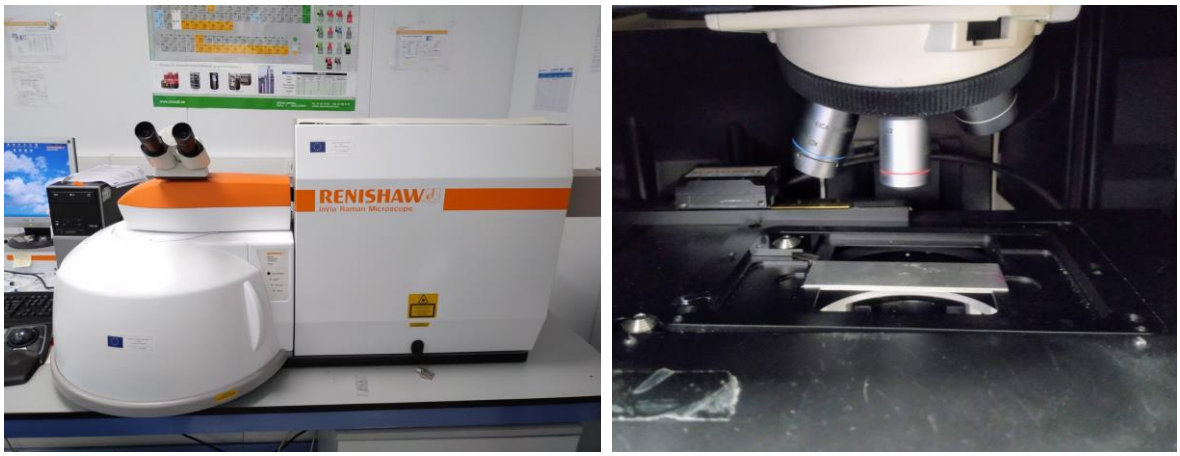

Figure 2.6. "InVia Reflex" Renishaw confocal Raman microscope. Image provided by the Research Support Services (RIAIDT) of the University of Santiago de Compostela.

X-ray diffraction: the crystallinity nanoparticles degree was characterized by X-ray diffraction (XRD) using a Philips type powder diffractometer fitted with a Philips W1710 control unit, a Vertical Philips "PW1820/00" goniometer and a FR590 Enraf Nonius generator. The instrument (Figure 2.7) was equipped with a graphite diffracted beam monochromator and a copper radiation source (λ(Kα1) = 1.5406Å), operating at 40 kV and 30mA. The X-Ray powder diffraction pattern (XRPD) has been collected by measuring the scintillation response to Cu Kα radiation versus the 2Θ value over a Θ range of 10-90, with a step size of 0.02 and counting time of 2 s per step.

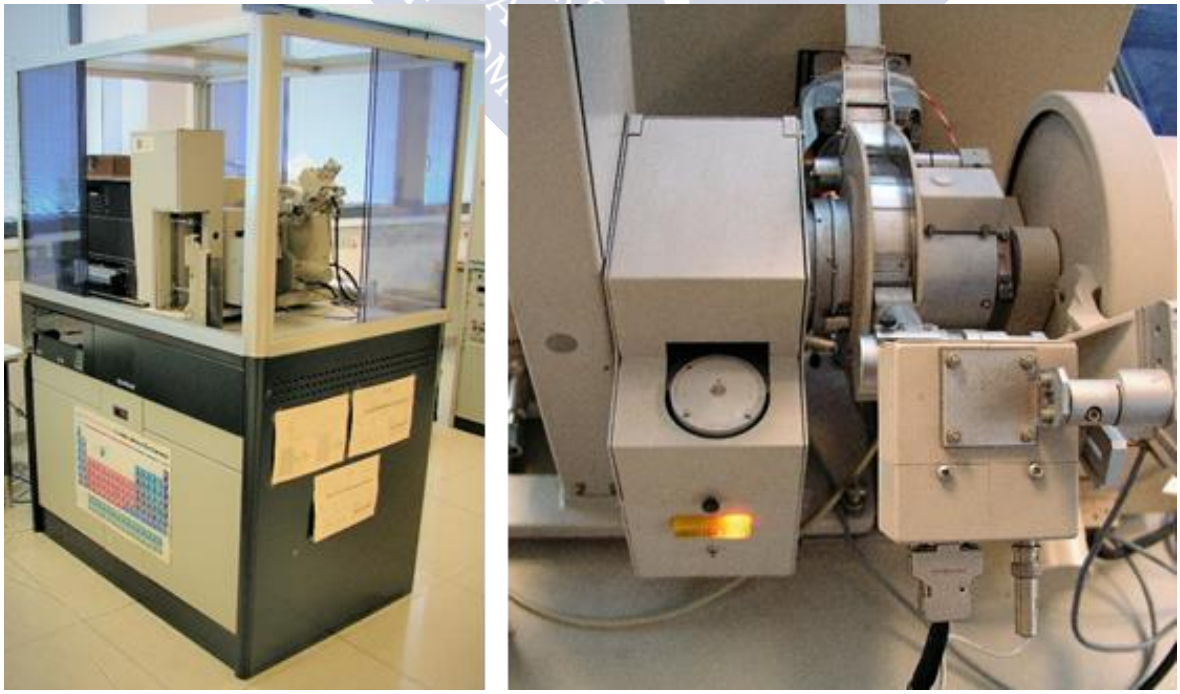

Figure 2.7. Philips type powder X-ray diffractometer: image taken from http://www.usc.es/gl/investigacion/riaidt/index.html.

2.2. Nanolubricants Preparation

The appropriate methodology for nanofluids preparation should be used with the goal of both, to guarantee their stability and to avoid the rupture of the nanoparticles structure. Two methods are usually utilized in the literature, the single-step and the two-step methods [2-5]. The single-step method combines the nanoparticles manufacturation with the synthesis of the nanofluid. The two-step method involves two procedures, firstly the nanoadditives synthesis and secondly, their dispersion in a base fluid. This method becomes the most economic for the nanofluids production in large scale [2,4]. In this PhD Thesis the two-steps method was used to prepare the nanolubricants, though in our case nanoparticles were provided by commercial source and not synthetized. The mass concentration of both components of the nanolubricants (base oil and nanoparticles) was determined by using a high precision Sartorius MC 210P microbalance (Figure 2.8). It is a polyrange microbalance, with different weighing capacities of 60/110/210 g. Its readability in the measured mass range is ± 0.00001 g.

To disperse the nanoparticles in the base oil two apparatus were used: an ultrasonic disruptor (HD 2200 Sonopuls) and an ultrasonic bath (Fisherbrand) (Figure 2.8). The sonicator probe of the disruptor conducts the acoustic energy from the transducer into the sample. The energy transferred to the nanolubricant depends on: the applied power, the total time that the dispersion is subjected to ultrasounds, the volume of the sample, the shape and diameter of the probe and its immersion depth. Sonication conditions used in this PhD Thesis were: power (200W), amplitude (302 μm), diameter and shape probe (MS73, 3mm) and sonication time (30 min). To minimize overheating during sonication process, the samples were immersed in an ice-water bath. The Fisherbrand ultrasonic bath (Figure 2.8) was used mainly to prepare nanolubricants based on graphene nanoplatelets. The following contidions were used: continuous shaking periods of 2 h, an ultrasonic power effective of 180 W and at a shaking frequency of 37 kHz. Another mixing system we have employed to disperse the nanolubricants is a mechanical Fisherbrand Vortex stirrer (Figure 2.8). The samples were shaken, after performing ultrasonic agitation, during continuous agitation periods of 10 minutes with around 16 rpm frequency. This equipment has different platform accessories to stir simultaneously several samples.

Figure 2.8. Different apparatus for nanolubricants preparation: a) High precision Sartorius MC 210P microbalance, b) mechanical Fisherbrand Vortex stirrer, c) Fisherbrand ultrasonic bath FB11203 and d) ultrasonic HD 2200 Sonopuls disruptor.

2.3. Nanolubricants Stability

To ensure stability is crucial for the final industrial application of nanolubricant. There are in the literature reviews [3,4,6-8] analysing the recent progress in both, the stability evaluation methods and the stability mechanisms. Nevertheless, these reviews are mainly focused on nanofluids for thermal applications. Hence, nanolubricants stability should receive greater attention by the scientific community in a near future [9,10]. The tendency of the nanoparticles to agglomerate, caused by their high surface energy, provokes a rapid sedimentation. For spherical nanoparticles Stoke´s law [8,10,11] relates the sedimentation speed (v), with the radius (r) and the density (ρ_{np}) of the nanoparticles, and with the density (ρ) and viscosity (η) of the base oil through the following expression:

$$v = \frac{2gr^2\left(\rho_{np} - \rho\right)}{9\eta} \tag{2.1}$$

Therefore, the nanolubricant stability depends strongly on the thermophysical properties of both base oil and nanoadditives, as well as the nanoparticle size. According to Stokes law, sedimentation speed is faster when the nanoparticle size increases, and when the difference between the density of the nanoparticle and the base oil is larger. To improve the stability, the use of surfactants and the nanoparticle surface modification could be used [3,4]. This PhD Thesis is not focused on the nanoparticle functionalization. We have only analyzed the employ of surfactants of different nature to improve the nanolubricants stability but we have not found a reduction on the sedimentation rate.

On the other hand various techniques, usually employed in the literature [5,8], were used in this PhD Thesis to analyse the stability of designed nanolubricants: visual control, UV–Vis spectrophotometry and dynamic light scattering (DLS). We have also analysed, for the first time, the potential use of a turbidimeter to control the stability. Finally, we have proposed a new method to control the sedimentation based on the temporal evolution of the refractive index.

Visual control

Direct visual observation, is the simplest and most commonly used method to initially evaluate stability of nanolubricants. In this PhD Thesis, once the nanolubricants were prepared, they were placed at room temperature without any disturbance. Subsequently, the samples were photographed every hour until detecting the nanoparticles sedimentation at the bottom of the container. Figure 2.9 shows the set-up used for the visual control.

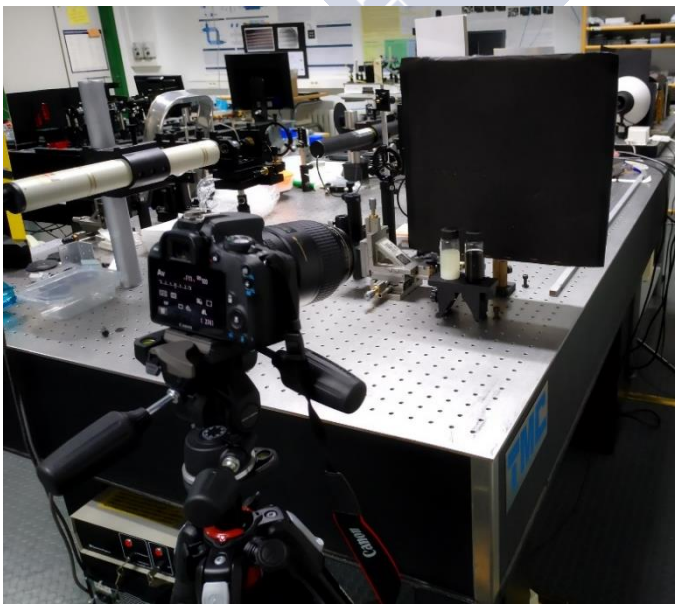

Figure 2.9. Set-up to performance the visual control method.

Three sedimentation process can take place in any unstable nanofluid [2]: dispersed sedimentation (the sediment height is gradually increased from the bottom as the solution become clearer), flocculated sedimentation (the sediment height decreases over time) and mixed sedimentation (both previous phenomena occur simultaneously). For all the nanolubricants formulated in the background of this PhD Thesis we have observed dispersed sedimentation.

Dynamic light scattering (DLS)

A Malvern Zetasizer Nano ZS analyser (Figure 2.10) was used to measure the nanoparticles size distribution and the average size of the aggregates. The temporal evolution of the average size gives information on the stability of nanolubricants. When the average size of nanoparticles or their aggregates keeps constant, the dispersion can be considered as stable. However, if average size decreases or increases with the time, sedimentation or agglomeration takes place, respectively. This equipment is a high performance molecular size analyser that can be used over a large concentration range. The experiments have been realized during research stays in the Applied Physics Department from the University of Vigo.

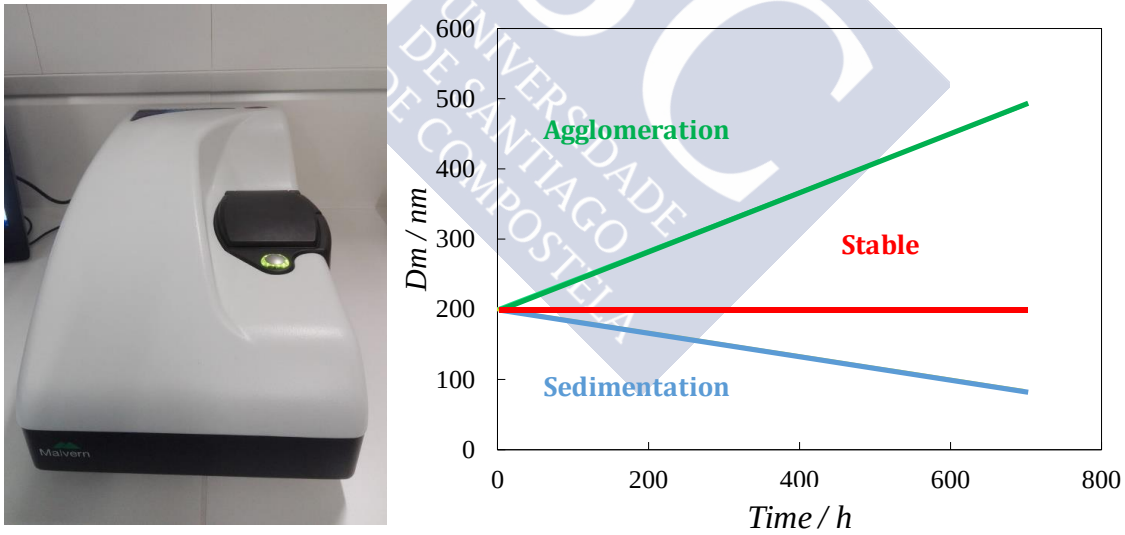

Figure 2.10. Malvern Zetasizer Nano ZS used to measure the nanoparticles size distribution.

Refractive index temporal evolution

In this PhD Thesis, we have proposed a new method to control the stability of nanolubricants. This method is based on the registration of the refractive index temporal evolution of a nanolubricant. We have not found previous works in the literature that use this procedure. A Mettler Toledo refractometer model RA-510M (Figure 2.11) with a

resolution of 1 10^{-5} was used. This apparatus can operate at any temperature between 288.15 K and 313.15 K. The measuring cell consists of a truncated and inverted cone-shaped cavity, with stainless steel walls, located on the upper part of the device. The base of this cone is a polished surface of a sapphire prism, on which the sample is placed. The cell has about 3 ml of capacity, but it is sufficient to introduce 0.2 ml in order to carry out the measurements. A black teflon flap cover is used to prevent the passage of outside light.

Figure 2.11. a) Mettler Toledo refractometer and b) nanoparticle sedimentation observed in the measuring cell.

Discarded techniques

As has been remarked above to analyse the stability of the nanolubricants other techniques were: UV–Vis spectrophotometry and temporal variation of turbidity. UV–Vis spectrophotometry is one of the most common techniques employed to investigate the stability of colloidal suspensions. In this PhD Thesis the stability of nanolubricants was studied with a Varian Cary 50 Bio UV–Vis spectrophotometer (Figure 2.12). The nanoadditive sedimentation is controlled trough the measurement of the absorbance, which is directly proportional to the nanoadditive concentration [12]. We have analysed the possibility to use the turbidity temporal evolution of the nanolubricant as a parameter to control the stability. For this aim a Hanna Instruments HI 88713 turbidimeter (Figure 2.12) was employed. Nevertheless, at the concentrations of interest (up to 2 wt %) signals from both devices (UV–Vis spectrophotometry and HI 88713 turbidimeter) show saturation

(nanolubricants are usually too opaque so that the absorbance and the turbidity cannot be analysed). Thus, it was necessary to dilute the dispersions up to a mass concentration around 10^{-3} wt %. We consider that it is not rigorous to extrapolate the behaviour of a nanolubricant from 10^{-3} wt % to 2 wt % nanoparticles concentration, and therefore both techniques have been discarded.

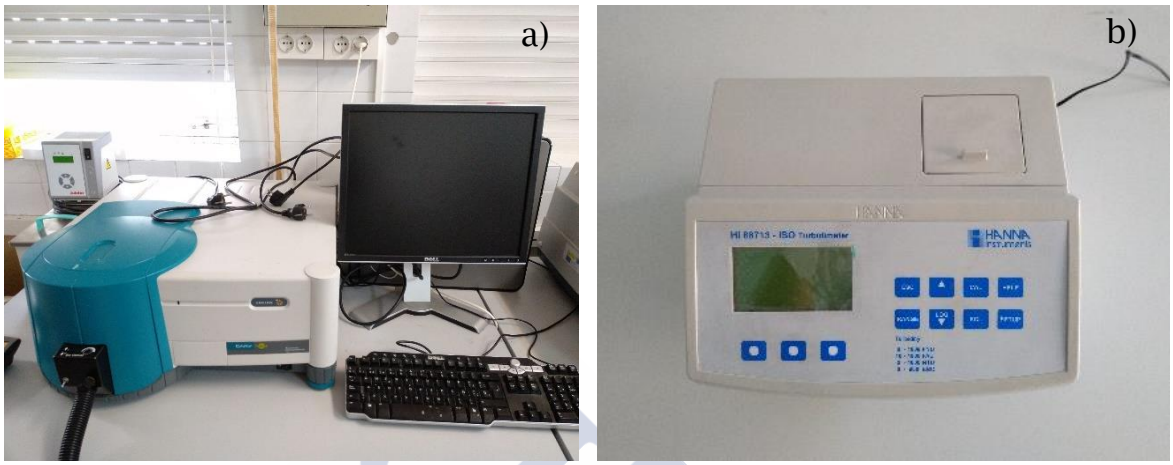

Figure 2.12. Discarded techniques employed to evaluate the stability of nanolubricants: a) Varian Cary 50 Bio UV–Vis spectrophotometer and b) Hanna Instruments HI 88713 turbidimeter.

Fourier transform infrared spectrometer (FTIR)

Fourier transform infrared spectroscopy (FTIR) analyses were conducted to study the formation of chemical bonds between nanoparticles and the base oils. For this aim, a FTIR VARIAN 670-IR spectrometer with a VARIAN microscope 610 IR mapping coupled was used (Figure 2.13). This apparatus is equipped with an ATR PIKE that allows to measure the absorbance spectra of nanoparticles.

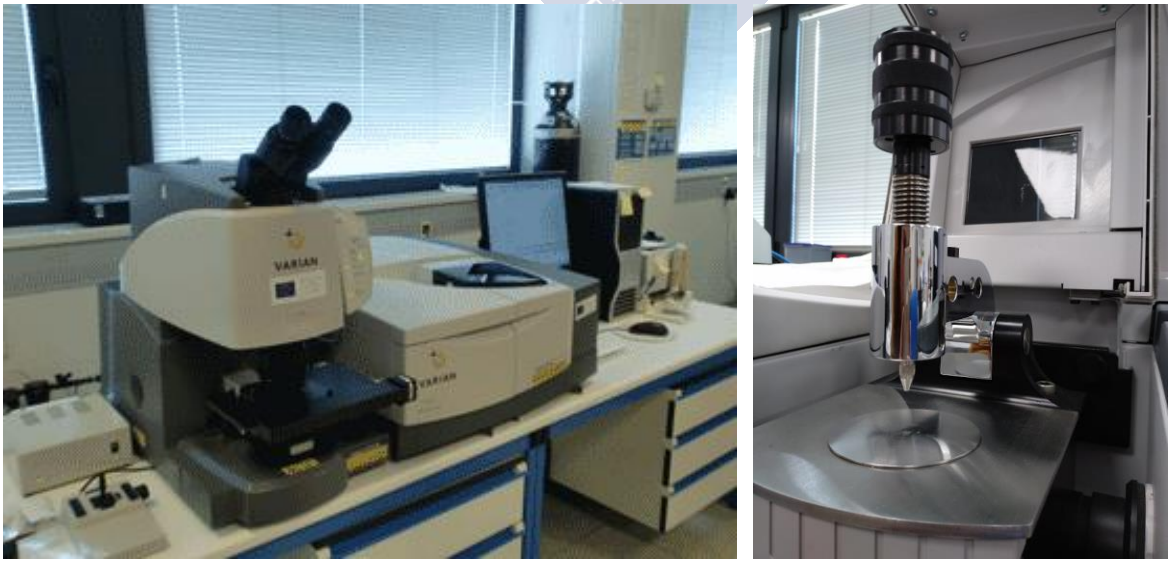

Figure 2.13. Fourier transform infrared FTIR VARIAN 670-IR spectrometer. Image provided by the Research Support Services (RIAIDT) of the University of Santiago de Compostela.

2.4. Thermophysical Characterization Techniques

In this section the description of the different apparatus used to characterize the thermophysical properties (density, dynamic and kinematic viscosity, viscosity index, speed of sound, rheological behavior and thermal conductivity) of the pure base oils and nanolubricants are presented.

Anton Paar Stabinger SVM 3000 viscometer

Density, viscosity and viscosity index of base oils and nanolubricants were measured with an Anton Paar Stabinger SVM 3000 (Figure 2.14). This device is composed of two cells, one for the viscosity measurement and another for density. Thus, Stabinger SVM 3000 allows measuring density, dynamic and kinematic viscosity from 233.15 K to 378.15 K, in a viscosity range from 0.2 mPa·s to 20 Pa·s. The operation principle of the Stabinger viscometer relies on rotating concentric cylinders, which is based on a modified Couette principle. Density cell is an oscillating glass U-tube, which is excited to produce mechanical resonant vibrations according to DIN 51757 standard. Both density and viscosity cells are filled at the same time, and the measurements are carried out simultaneously. The temperature of the cell is controlled through an integrated thermostat with cascaded Peltier elements and measured with a Pt100 thermometer with an expanded (k = 2) uncertainty of 0.02 K. Experimental expanded (k = 2) uncertainties of 1 % and 0.05 % have been estimated for dynamic viscosity and density, respectively.

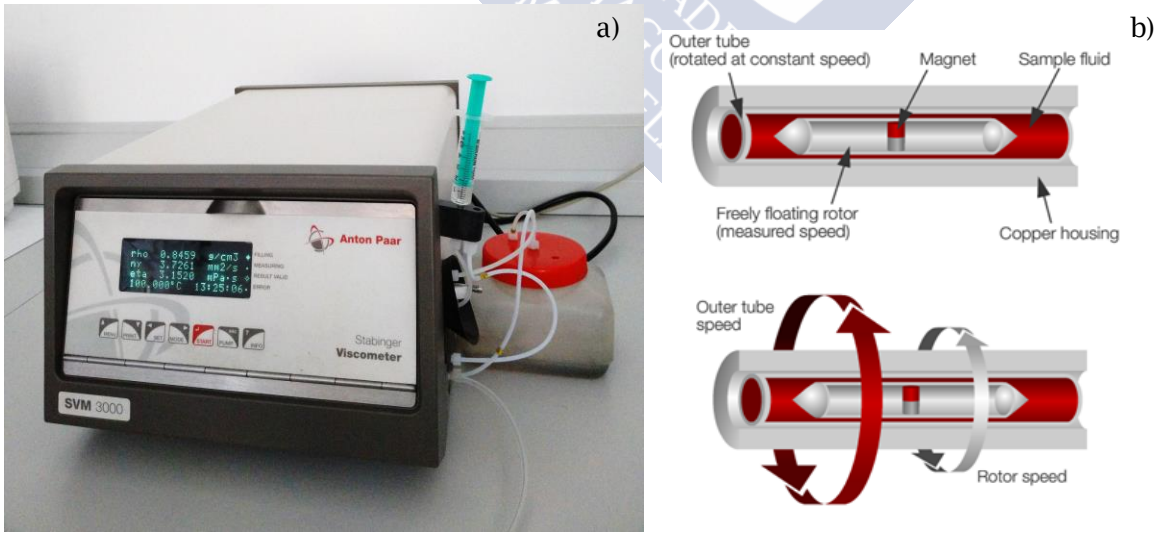

Figure 2.14. Anton Paar Stabinger SVM 3000 viscometer: a) device and b) diagram of the operation principle.

Measurements were performed automatically in the temperature range scan mode, from 278.15 K to 373.15 K with a step of 5 K, at atmospheric pressure. The results are displayed on a LCD screen and transferred to the internal data memory. The required sample volume is 2.5 cm^3. Cleaning is performed immediately after measurements with the suitable solvent for each sample, usually n-hexane, petroleum ether or acetone. Anton Paar Stabinger viscometer can be used to determine the viscosity index according to ASTM D2270/ISO 2909. Viscosity index (VI) is a dimensionless number which measures the variation of viscosity with the temperature. During the machinery operation temperature changes occur so, to ensure the optimal lubrication it is important to know the temperature dependence of the oil viscosity. Thus, VI is usually used to characterize the viscosity-temperature behavior of lubricants.

Anton Paar DSA 5000 densimeter

Density and sound speed of base oils and nanolubricants have also been measured using another Anton Paar vibrating tube densimeter DSA 5000 (Figure 2.15). This apparatus can operates from (283.15 to 338.15) K at atmospheric pressure. The upper limit for the standard uncertainty of density measurements (samples with viscosity higher than 100 mPa·s) performed with DSA 5000 is 0.0002 $g \cdot cm^{-3}$. For samples with a viscosity lower than 30 mPa·s, a standard uncertainty of 0.00004 $g \cdot cm^{-3}$ is obtained. The speed of sound was also measured (at an operating frequency of approximately 3 MHz) with a standard uncertainty of 2 $m \cdot s^{-1}$. Density measurements obtained with DSA 5000 densimeter were compared with those measured with Anton Paar Stabinger SVM 3000 with the aim to check the consistency of the experiments. This fact is of major importance for nanolubricants with lower stability.

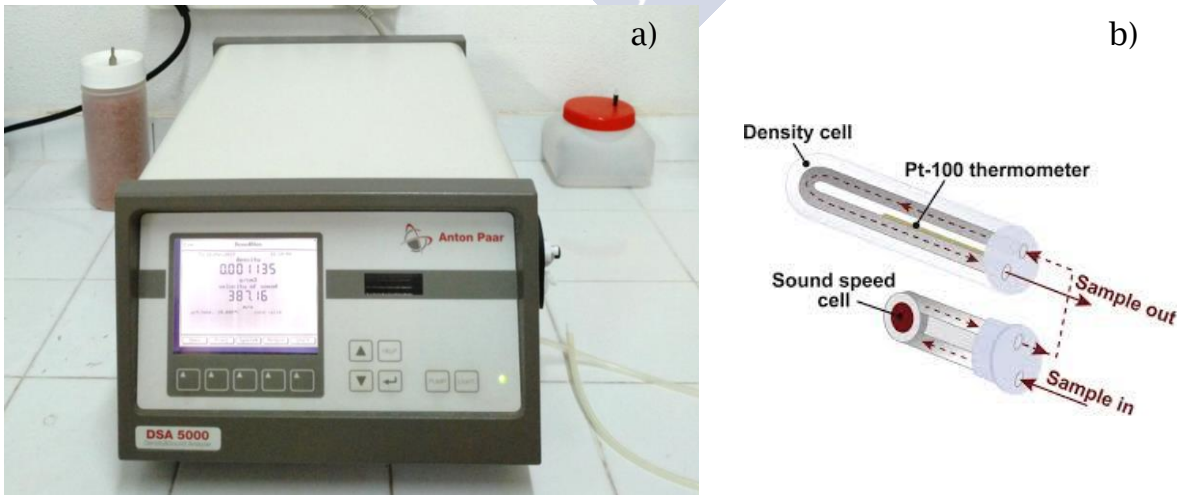

Figure 2.15. Anton Paar DSA 5000 densimeter: a) device and b) operation scheme of measuring cells [13].

Anton Paar rheometer Physica MCR 101

Rheological tests can be mainly classified into rotational or oscillatory analysis. Flow tests are used to study the viscosity dependence with shear rate (pseudoplastic or dilatant behaviours) and/or time (thixotropic or rheopectic behaviours). Rheological behaviour of some nanolubricants and base oils studied in this PhD Thesis were determined using an Anton Paar rotational Physica MCR 101 rheometer (Figure 2.16). This apparatus is equipped with a cone-plate geometry with a cone diameter of 25 mm and a cone angle of 1°. This device allows controlling torques between (0.5 to $125 \cdot 10^3$) μN·m and normal forces from (0.1 to 30) N, with resolutions of 0.002 μN·m and 0.02 N, respectively. The measurement consists of imposing a shear stress to the sample and recording the related shear rate. Temperature is controlled with a Peltier P-PTD 200 system/device (diameter of 56 mm) placed at the lower plate, with an uncertainty of 0.02 K [14,15]. Flow curves test for base oils and the nanolubricants were performed between (283.15 - 323.15) K with a step of 10 K using controlled shear stress operation mode. To obtain the dynamic viscosity, three replicates at each experimental condition were carried out. The experiments have been realized in collaboration with the Applied Physics Department from the University of Vigo.

Figure 2.16. Anton Paar Physica MCR 101 rheometer: a) device and b) used CP25-1 geometry.

KD2 Pro Thermal Properties Analyzer

Thermal conductivity was determined using a KD2 Pro Thermal Properties Analyzer (Decagon Devices) in the temperature range from 266 K to 333 K. This apparatus (Figure 2.17) has an operation principle based on the transient hot-wire method [16]. The apparatus consists of a handheld microcontroller and a KS-1 sensor needle (1.3 mm diameter and 60 mm length) which can measure thermal conductivities from (0.02 to 2) $W \cdot m^{-1} \cdot K^{-1}$. An expanded uncertainty was estimated lower than 0.01 W m^{-1} K^{-1} for the range (0.02 to 0.2) W m^{-1} K^{-1} and 3% for (0.2 to 2) W m^{-1} K^{-1} [17]. To ensure a uniform initial temperature, nanolubricants were fully immersed in a Grant GP200 (Grant Instruments) oil bath.

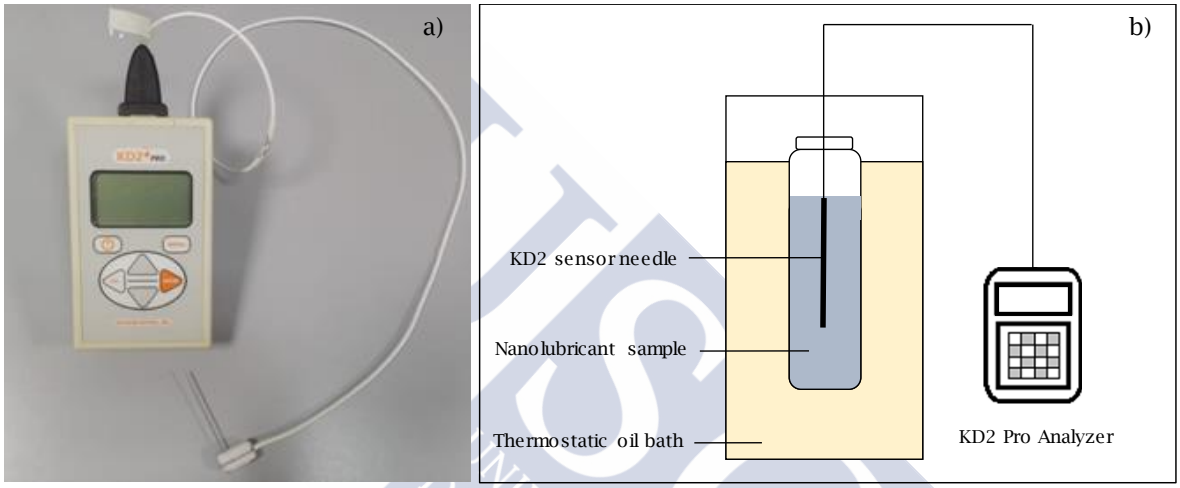

Figure 2.17. KD2 Pro Thermal Properties Analyzer: a) device and b) experimental set-up.

Anton Paar DMA HPM densimeter

Volumetric behaviour at high pressure of several pure base oils was determined by means of an Anton Paar DMA HPM vibrating tube densimeter. This apparatus can operate over a temperature range from 263.15 K to 473.15 K and at pressures up to 140 MPa. This densimeter consists in two units, an electronic processing unit (mPDS 2000V3) and a high pressure measuring cell (DMA HPM). The first one excites the U-tube at constant amplitude and indicates the vibration period with seven significant digits. The high pressure measuring cell contains the vibrating tube. This equipment is fully automated except the operations of filling and cleaning. Figure 2.18 shows a diagram of the automated densimeter DMA HPM experimental set-up. This densimeter is connected to a pressure line (tubing and valves), a piston pressure intensifier (HiP 50-5.75-30) and a pressure transducer (HBM Digibar II K-PE3000). The set-up also includes a thermostatic bath (Polyscience 9102) and a Pt100 probe. Temperature data acquisition is carried out by an Agilent 34970A unit remotely controlled

via IEEE 488 with a PC. The control system and data acquisition are performed by means of Agilent VEE Pro 7.0 software.

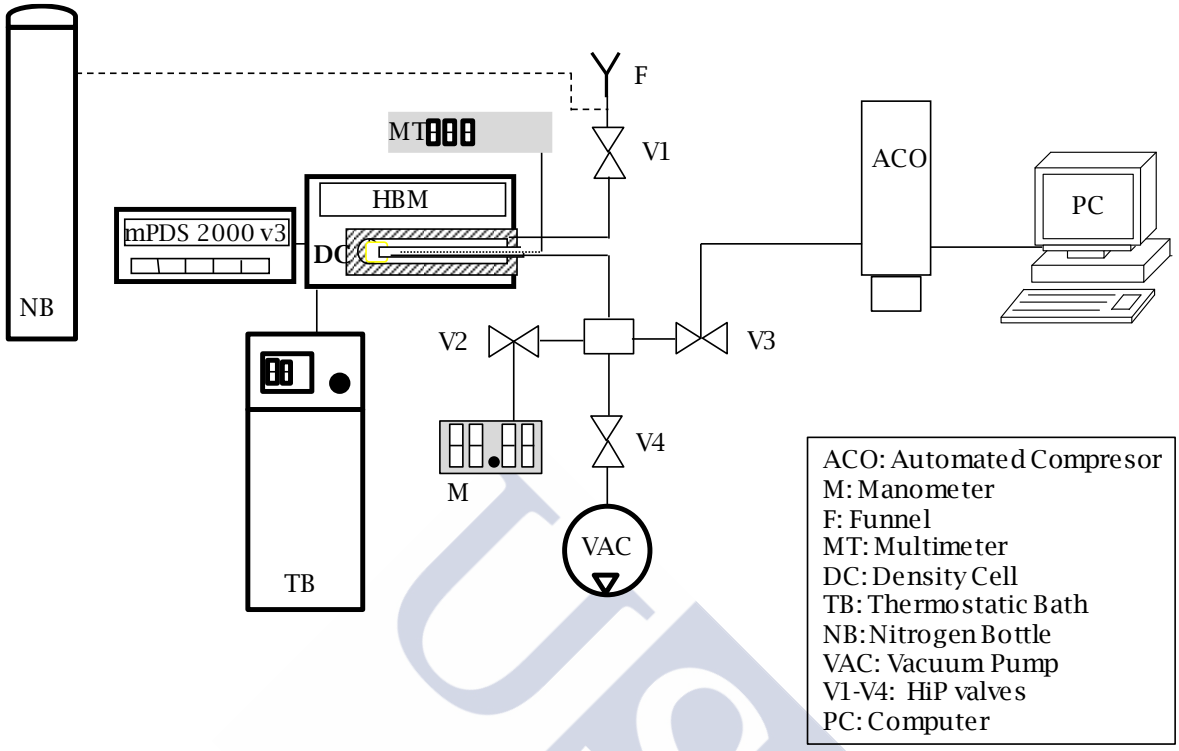

Figure 2.18. Scheme of the DMA HPM Anton Paar densimeter experimental set-up.

In this PhD Thesis, density measurements were performed in the temperature range from 278.15 to 398.15 K. The temperature and pressure uncertainties are ± 0.02 K and ± 0.02 MPa, respectively. The calibration was performed with vacuum, Milli-Q water, and n-decane following the procedure proposed by Comuñas *et al.* [18]. The expanded density uncertainties were estimated [19] considering the uncertainties of the temperature, pressure, water and decane density, and oscillation period measurements for water, decane, vacuum, and the measured liquid. Hence, the expanded uncertainties (k = 2) of the density are ± 0.7 kg m^{-3} for temperatures below T = 373.15 K and pressures up to 120 MPa, ± 5 kg m^{-3} at T = (373.15 and 398.15) K and p = 0.1 MPa, and ± 3 kg m^{-3} at $T \geq 373.15$ K and $p > 0.1$ MPa. Reliability of the apparatus and its calibration were tested by measuring density of *n*-decane. Absolute average deviation (AAD%) of 0.07% and 0.05% were obtained between the experimental density data and values reported by Cibulka and Hnědkovsky [20] and by Lemmon and Span [21], respectively.

Falling body viscometer VisLPT1

Viscosities at high pressure of TMPTO base oil were measured using a falling body viscometer, VisLPT1, which can operate at pressures up to 150 MPa. The measuring cell is made up of concentric cylindrical tubes. The liquid under study is introduced firstly in the inner tube and then in the space between them, so that the pressure is the same on both sides of the inner tube, avoiding a possible deformation of the tube linked to a pressure gradient. Figure 2.19 shows a scheme of this equipment. The viscometer cell is covered by an aluminum frame where a heat-carrying fluid (silicone oil) is circulating. The temperature is regulated using a Lauda Proline RP 1840 thermostat and it is measured with a thermocouple located inside the cell, in contact with the sample, with an uncertainty of ± 0.5 K. The liquid is compressed by means of a HiP compressor (model 50-5.75-30) and the pressure is measured by a transducer (HBM P3MB) and a numeric indicator (HBM Scout 55) with an accuracy of ± 0.2 MPa. A pneumatic device connected to an air compressed inlet allows rotating the cell an angle of 180º around the horizontal axis.

A cylindrical magnetic steel sinker (6.10 mm of diameter, 20 mm of length and 7.695 g cm^{-3} of density at 298.15 K and 0.1 MPa) with a hemispherical end falls vertically through the sample. Four electrical coils are fixed to the outer tube, detecting the passage of the sinker through a variation of the magnetic flux. When the sinker passes through a coil, the induced signal exhibits a maximum triggering in an electronic timer (Chronoprinter 520, TAG Heuer) and the time (t) that takes the sinker to travel the distance between two consecutive coils is measured. Thus, we obtain three time intervals associated with the passage of the falling body through the four coils. By comparison of these three time intervals we can verify that the body reached the terminal velocity.

The measuring principle of a falling body viscometer is based on the relationship between the fluid viscosity (η) and the time (t) that a solid takes to fall inside the inner tube through the fluid (once it has reached its terminal velocity under conditions of laminar flow) [22]. The working equation employed in this work is:

$$\eta(p,T) = \frac{t(1-\rho/\rho_s)}{A\left[1+2\alpha_{vt}(T-T_{ref})\right]\left[1-2\beta_{vt}(p-p_{ref})/3\right]} \tag{2.2}$$

where t is the falling time, ρ and ρ_s are the density for the fluid and for the sinker, respectively, at the temperature T and pressure p. A is a calibration constant, and α_{vt} and β_{vt}, are the coefficients of expansion and compressibility of the viscometer tube (INCONEL 718) at reference conditions T_{ref} = 298.15 K and p_{ref} =0.1 MPa. This equation presents the

advantage that the parameter *A* is not dependent on either pressure or temperature. Therefore, the calibration procedure can be performed at atmospheric pressure with certificated standard oils.

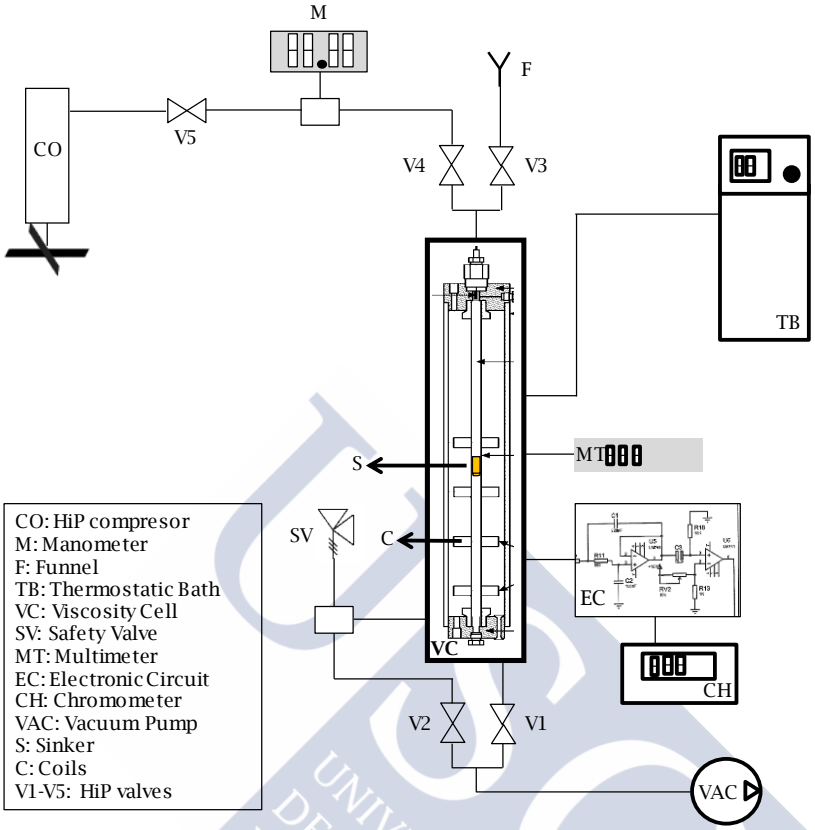

Figure 2.19. Scheme of the falling body viscometer (VisLPT1) for high pressures experimental set-up.

Density of the sinker for each *p* and *T* condition is calculated with the following equation:

$$\rho_s(p,T) = \frac{\rho_s(p_{ref},T_{ref})}{\left[1+3\alpha_s(T-T_{ref})\right]\left[1-\beta_s(p-p_{ref})\right]} \tag{2.3}$$

where α_s and β_s are the coefficients of expansion and compressibility of the sinker (X4CrNiMo16-5-1) at reference conditions T_{ref} = 298.15 K and p_{ref} = 0.1 MPa. Values of the expansion coefficients are α_s =10.8·10^{-6} K^{-1} and α_{vt} =12.8·10^{-6} K^{-1}, respectively, whereas for compressibility we have β_s =5·10^{-6} MPa^{-1} and β_{vt} =4.8·10^{-6} MPa^{-1}. In this PhD Thesis calibration constant *A* for equation (2.2) was estimated from three Cannon certified oils at atmospheric pressure from 293.15 to 353.15 K. These fluids cover the viscosity range from 14.5 mPa s for Cannon N75 up to 1482 mPa s for Cannon S600. The value of the calibration constant *A* is 1.206 ± 0.003 Pa^{-1}. Taking into account uncertainties of temperature, pressure, falling times, calibration constant and densities of both sinker and fluid, the uncertainty of the device is estimated to be ± 3.5% with a coverage factor *k*=2.

2.5. Tribological Characterization Techniques

Tribological characterization of the formulated nanolubricants and of the base oils was performed and compared with the aim to analyse the ability of the nanoadditives as potential friction and anti-wear improvers. In this section, we present a description of the different techniques used to determine the friction coefficients, wear and Stribeck curves.

CSM Standard Tribometer

To obtain the friction coefficients for each nanolubricant and pure base oil, tribological tests were performed on a tribometer CSM Standard with a reciprocating ball-on-plate configuration (Figure 2.20). A 100Cr6 steel ball and an AISI 420 stainless steel plate were used. Before starting a test, the ball and the plate are cleaned in hexane and dried with warm air. Then, the ball is introduced and tightly fixed in its holder, where it cannot rotate and thus, the contact will be in pure sliding. The plate is clamped to the part of the tribometer which will be in linear reciprocating movement during the test. The ball-holder is then fixed in the measuring arm, so the ball will remain vertically in contact with the plate. Five drops of the studied nanolubricant are added to the interface (plate/ball) subsequently the selected load is placed on the ball holder. During the test, the displacements of the measuring arm in the direction of the movement are detected by an inductive displacement transducer. This signal is recorded and converted by the software into the friction coefficient throughout the experiment. At the end of the test, the plate and the ball are rinsed with acetone and hexane.

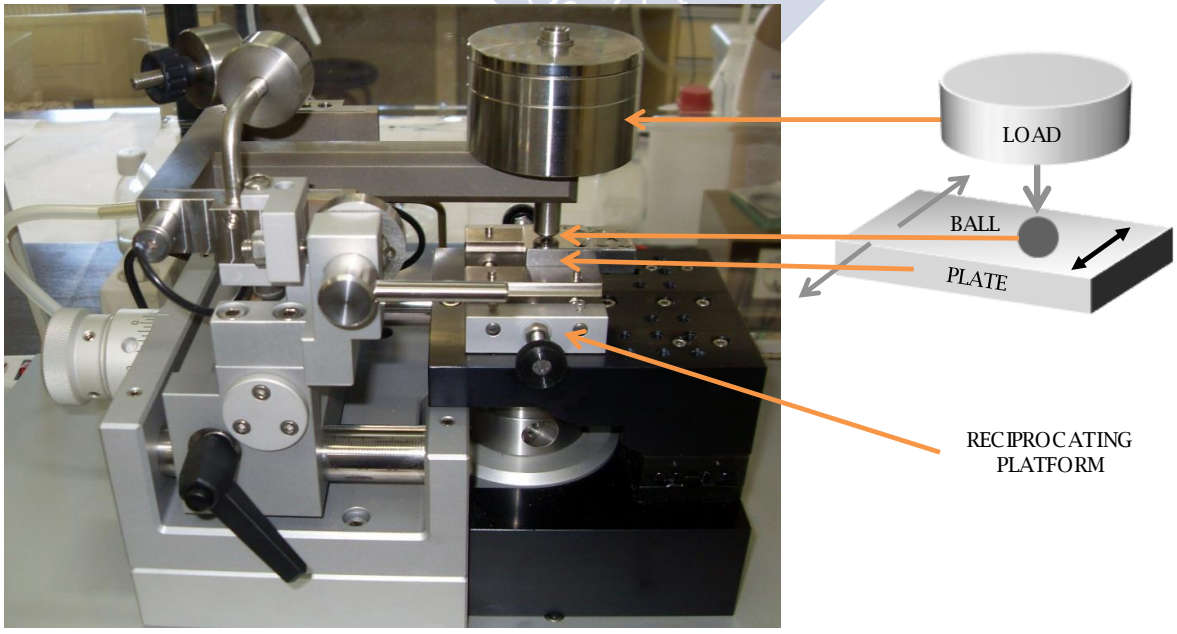

Figure 2.20. CSM Standard tribometer with reciprocating ball-on-plate configuration.

All the measurements were performed at room temperature, with a stroke of 10 mm, at a maximum sliding speed of 0.1 m s^{-1}, for a total sliding distance of 500 m (stop condition) and a duration of around 7850 s. Two different loads (2.5 and 5 N) were considered for the tribotest corresponding to the base oils and the nanolubricants. At least three replicates were performed for each operation condition, so the friction coefficient reported is an average of these results. The criterion considered for selecting values was that, the difference of the friction coefficient of a test compared to the mean value should be below 15 % [23].

Film Measurement System EHD2

Film thickness measurements were determined using a ball-on-disc test apparatus (PCS Instruments, model EHD2) equipped with optical interferometry (Figure 2.21). The load-applying system is based on moving a steel ball (19.05 mm of diamater) against the rotating glass disc (Figure 2.21). The ball is made from carbon chrome steel and has a high polished grade to ensure good reflectivity. The standard glass disc is coated with approximately 20 nm of chromium and 500 nm of silica layer and can be tested up to approximately 50 N of load (corresponding with maximum Hertz pressure of 0.66 GPa). The disc and the steel ball are controlled by two electric motors for performing tests under rolling/sliding conditions. The system can accurately calculate the central film thickness from measuring the wavelength of the light returned from the central plateau of the contact [24,25].

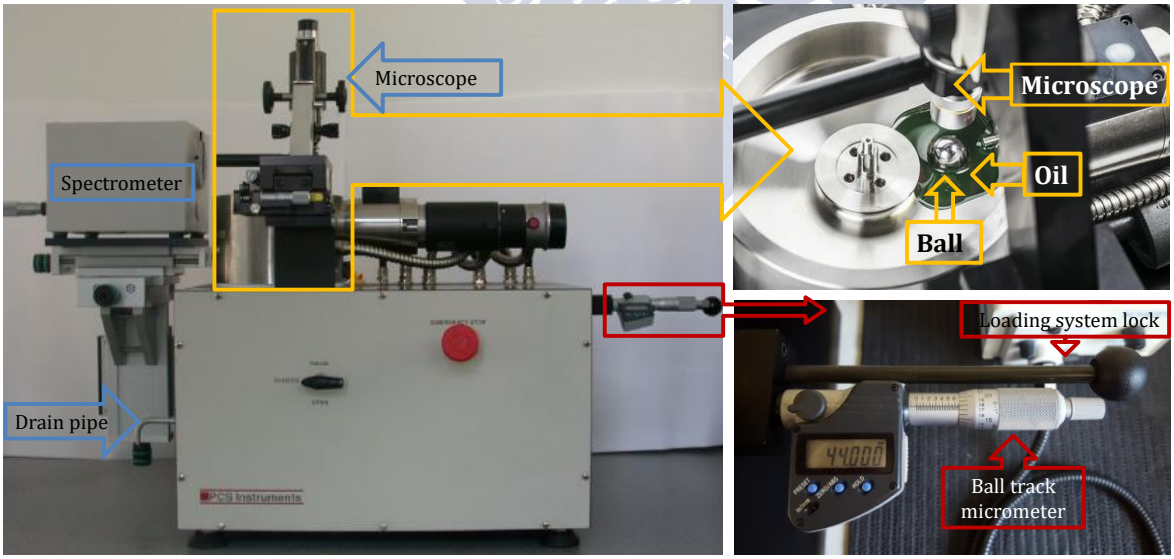

Figure 2.21. Film measurement system EHD2 equipped with optical interferometry.

This apparatus was also used in this PhD Thesis to determine the friction coefficients. In this case, we use the same ball than that used in the film thickness measurements. Steel

discs (100 mm diameter) with different roughness were used: a polished disc and two rough discs with initial roughness (*Ra*) of 0.1 μm and 0.5 μm (Figure 2.22). The applied load generates contact pressures up to 1.11 GPa. The lubricant film thickness and friction coefficient tests were made under fully flooded lubrication (120 ml of lubricant sample) and three operating temperatures (303.15, 333.15 and 353.15 K) were used. The lubricant film thickness tests were performed at 5% slide-to-roll ratio (SRR) while the friction coefficient at 5% and 50% SRR. In both cases the entrainment speed ranges from 0.04 to 2 m s^{-1}.

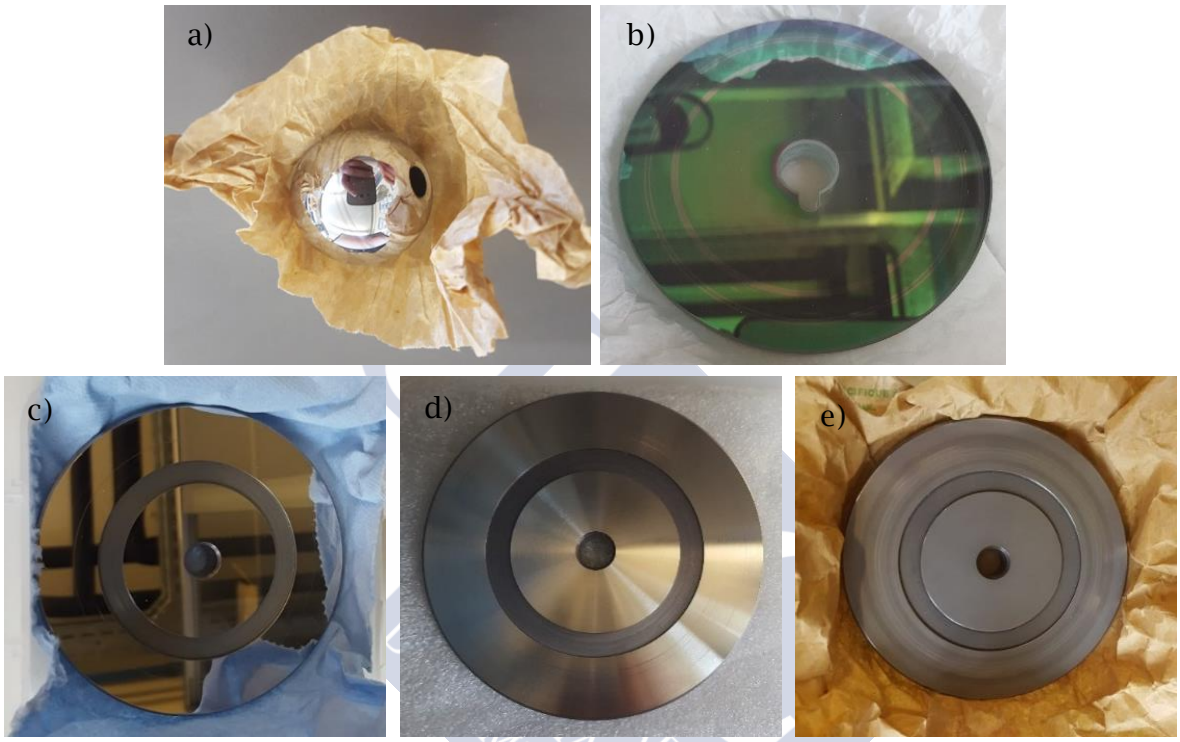

Figure 2.22. Specimens used to determine lubricant film thickness and friction coefficient: a) steel ball, b) glass disc, c) polished disc, d) rough disc *Ra* = 0.1 μm and e) rough disc *Ra* = 0.5 μm.

3D Optical Profiler Sensofar S Neox

A 3D Optical Profiler Sensofar S Neox (Figure 2.23) was employed to measure the roughness of the worn surfaces. This equipment can be used in three different modes, confocal, interferometry and focus variation mode. The suitable mode is selected according to specifications of the studied plate. For these measurements, confocal mode with a 10X objective was used to analyse the roughness of the worn surface of the plates lubricated with both, the base oil and the nanolubricants. Confocal mode has a vertical resolution of 25 nm and a maximun slope of 14 º when a 10X objective is used [26]. The roughness parameter (*Ra*) was determined accordingly to the ISO 4287 standard applying a Gaussian filter with a long wavelength cut-off of 0.08 mm.

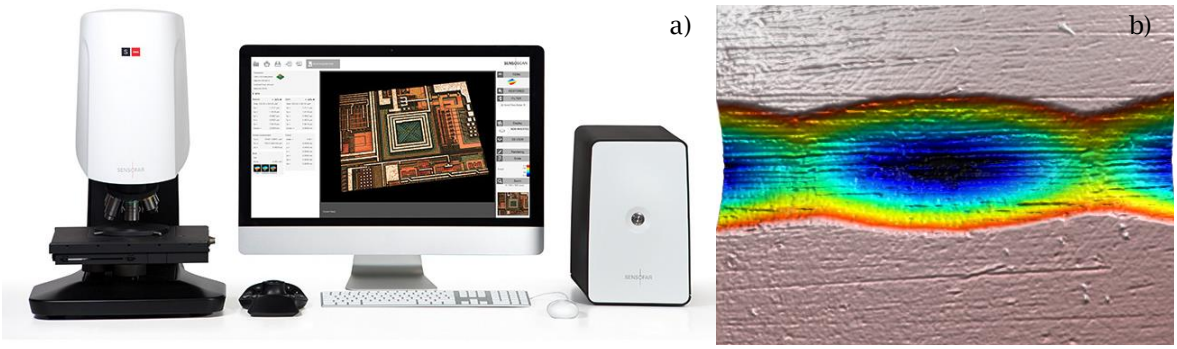

Figure 2.23. 3D Optical Profiler Sensofar S Neox: a) device and b) wear scar of TMPTO.

The surface of the worn track created on the plates after the tribotest was analysed by surface electron microscopy (SEM) at a magnification of 200 μm. The scanning electron microscope scans the ball and plate surface with an electrons beam and detects the emitted signals. Then, this information is converted into a surface image. These analyses were performed by the Research Support Services of the University of Santiago de Compostela with a Carl Zeiss FESEM ULTRA Plus Scanning Electron Microscope (Figure 2.4).

2.6. Processing

The process flow diagram employed in this PhD Thesis to optimize the characterization of the thermophysical and tribological properties of pure base oils and nanolubricants is presented in Figure 2.24. The methodology consists in a sequence of five steps: characterization (1), nanolubricant preparation (2), stability method assessment (3), thermophysical properties determination (4), and finally tribological performance (5). Direction of flow from one step to another is indicated in the Figure 2.24. Mainly the condition to reach steps 4 and 5 is to obtain nanolubricants with temporal stability larger than the time needed to perform the experiments (film thickness determination, friction tests, viscosity and density measurements and rheological behaviour, among others).

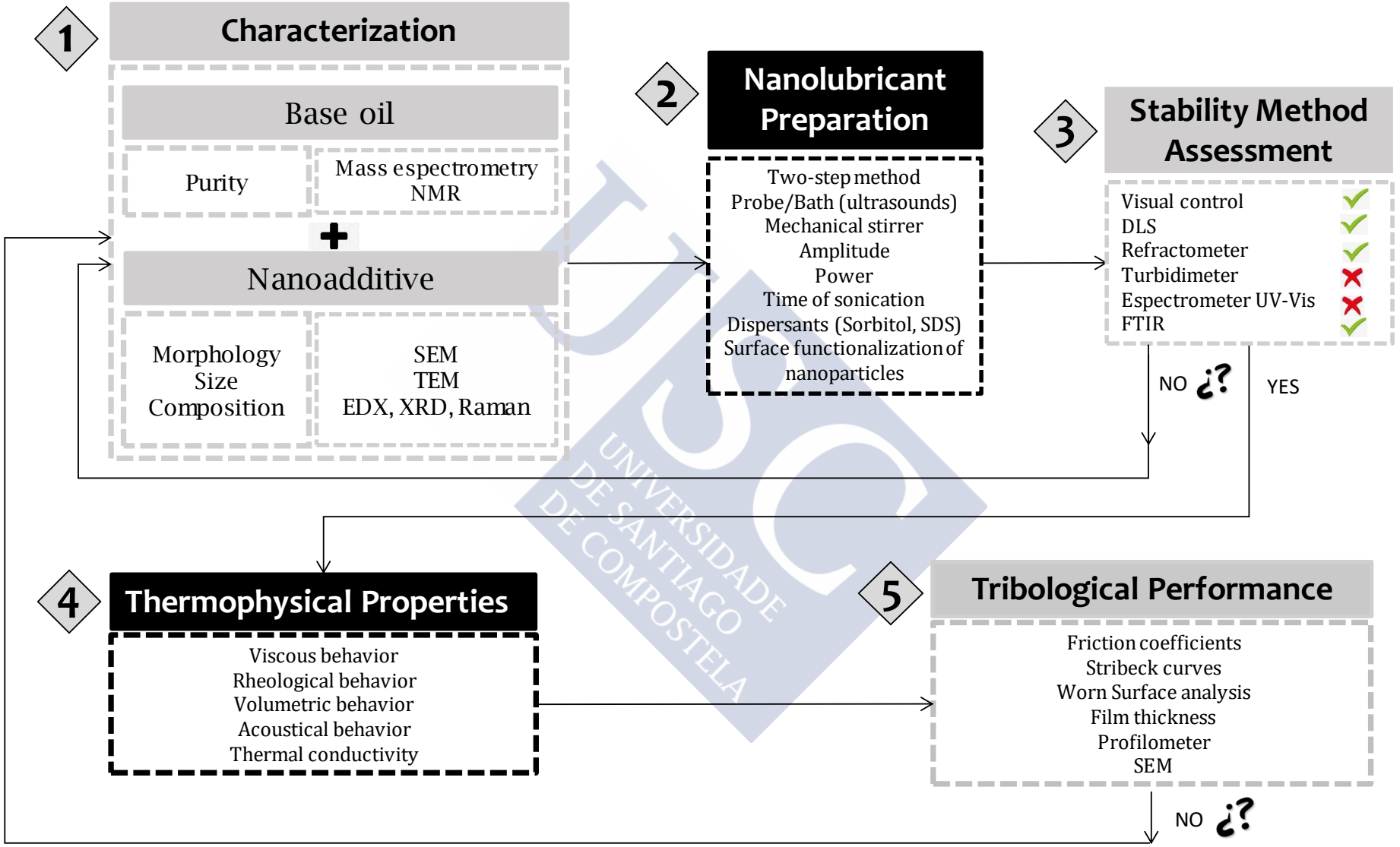

Figure 2.24. Flow diagram used for the thermophysical and tribological characterization of nanolubricant.

2.7. References

[1] W. Dai, B. Kheireddin, H. Gao, H. Liang, Roles of nanoparticles in oil lubrication, Tribol. Int. 102 (2016) 88-98.

[2] S.U. Ilyas, R. Pendyala, N. Marneni, Preparation, Sedimentation, and Agglomeration of Nanofluids, Chem. Eng. Technol. 37 (2014) 2011-2021.

[3] W. Yu, H. Xie, A Review on Nanofluids: Preparation, Stability Mechanisms, and Applications, J. Nanomater. 2012 (2012) 17.

[4] L. Kong, J. Sun, Y. Bao, Preparation, characterization and tribological mechanism of nanofluids, RSC Advances 7 (2017) 12599-12609.

[5] Y. Li, J.e. Zhou, S. Tung, E. Schneider, S. Xi, A review on development of nanofluid preparation and characterization, Powder Technol. 196 (2009) 89-101.

[6] S. Mukherjee, S. Paria, Preparation and Stability of Nanofluids-A Review, J. Mech. Civ. Eng. 9 (2013) 63-69.

[7] D. Wen, G. Lin, S. Vafaei, K. Zhang, Review of nanofluids for heat transfer applications, Particuology 7 (2009) 141-150.

[8] A. Ghadimi, R. Saidur, H.S.C. Metselaar, A review of nanofluid stability properties and characterization in stationary conditions, Int. J. Heat Mass Transfer 54 (2011) 4051-4068.

[9] Y. Chen, P. Renner, H. Liang, Dispersion of Nanoparticles in Lubricating Oil: A Critical Review, Lubricants 7 (2019) 7.

[10] N.F. Azman, S. Samion, Dispersion Stability and Lubrication Mechanism of Nanolubricants: A Review, Int. J. Precis. Eng. Manuf.- Green Technol. 6 (2019) 393-414.

[11] H. Chang, Z.Y. Li, M.J. Kao, K.D. Huang, H.M. Wu, Tribological property of TiO_2 nanolubricant on piston and cylinder surfaces, J. Alloys Compd. 495 (2010) 481-484.

[12] Y. Hwang, J.K. Lee, C.H. Lee, Y.M. Jung, S.I. Cheong, C.G. Lee, B.C. Ku, S.P. Jang, Stability and thermal conductivity characteristics of nanofluids, Thermochim. Acta 455 (2007) 70-74.

[13] T.J. Fortin, A. Laesecke, M. Freund, S. Outcalt, Advanced calibration, adjustment, and operation of a density and sound speed analyzer, J. Chem. Thermodyn. 57 (2013) 276-285.

[14] D. Cabaleiro, M.J. Pastoriza-Gallego, C. Gracia-Fernández, M.M. Piñeiro, L. Lugo, Rheological and volumetric properties of TiO_2-ethylene glycol nanofluids, Nanoscale Res. Lett. 8 (2013) 286.

[15] D. Cabaleiro, M.J. Pastoriza-Gallego, M.M. Piñeiro, L. Lugo, Characterization and measurements of thermal conductivity, density and rheological properties of zinc oxide nanoparticles dispersed in (ethane-1,2-diol+water) mixture, J. Chem. Thermodyn. 58 (2013) 405-415.

[16] G. Paul, M. Chopkar, I. Manna, P.K. Das, Techniques for measuring the thermal conductivity of nanofluids: A review, Renew. Sustain. Energy Rev. 14 (2010) 1913-1924.

[17] D. Cabaleiro, M.J. Pastoriza-Gallego, M.M. Piñeiro, J.L. Legido, L. Lugo, Thermophysical properties of (diphenyl ether+biphenyl) mixtures for their use as heat transfer fluids, J. Chem. Thermodyn. 50 (2012) 80-88.

[18] M.J.P. Comuñas, J.-P. Bazile, A. Baylaucq, C. Boned, Density of Diethyl Adipate using a New Vibrating Tube Densimeter from (293.15 to 403.15) K and up to 140 MPa. Calibration and Measurements, J. Chem. Eng. Data 53 (2008) 986-994.

[19] J.J. Segovia, O. Fandiño, E.R. López, L. Lugo, M.C. Martín, J. Fernández, Automated densimetric system: Measurements and uncertainties for compressed fluids, J. Chem. Thermodyn. 41 (2009) 632–638.

[20] I. Cibulka, L. Hnědkovský, Liquid Densities at Elevated Pressures of *n*-Alkanes from C_5 to C_{16}: A Critical Evaluation of Experimental Data, J. Chem. Eng. Data 41 (1996) 657-668.

[21] E.W. Lemmon, R. Span, Short Fundamental Equations of State for 20 Industrial Fluids, J. Chem. Eng. Data 51 (2006) 785-850.
[22] J. Kestin, W.A. Wakeham, Transport Properties of Fluids: Thermal Conductivity, Viscosity, and Diffusion Coefficient, 1st ed., Hemisphere Publishing Corporation, New York, 1988.
[23] I. Minami, T. Inada, R. Sasaki, H. Nanao, Tribo-Chemistry of Phosphonium-Derived Ionic Liquids, Tribol. Lett. 40 (2010) 225-235.
[24] A. Hernández Battez, C.M.C.G. Fernandes, R.C. Martins, M. Bartolomé, R. González, J.H.O. Seabra, Two phosphonium cation-based ionic liquids used as lubricant additive: Part I: Film thickness and friction characteristics, Tribol. Int. 107 (2017) 233-239.
[25] https://pcs-instruments.com/wp-content/uploads/2014/03/EHD2-Brochure2017.pdf. 2017.
[26] https://www.sensofar.com/metrology-2/sneox/specifications/. 2017.

USC
UNIVERSIDADE
DE SANTIAGO
DE COMPOSTELA

3. RESULTS SUMMARY

USC
UNIVERSIDADE
DE SANTIAGO
DE COMPOSTELA

3. RESULTS SUMMARY

3.1. General Discussion

This chapter reports the results obtained in this PhD Thesis on the thermophysical and tribological properties of different base oils and several tailor-made nanolubricants. We present the articles that have been published in international journals, indexed in the Journal Citation Reports, which are classified in the first quartile (Q1). We include two articles that will be soon submitted for publication. Moreover, the communication and proceedings presented at scientific conferences are also listed.

Publications in international journals:

[1] M.J.G. Guimarey, M.J.P. Comuñas, E.R. López, A. Amigo, J. Fernández. Volumetric behavior of some motor and gear-boxes oils at high pressure: compressibility estimation at EHL conditions. Ind. Eng. Chem. Res., 2017, 56, p. 10877–10885
DOI: 10.1021/acs.iecr.7b02002

[2] M.J.G. Guimarey, M.R. Salgado, M.J.P. Comuñas, E.R. López, A. Amigo, D. Cabaleiro, L. Lugo, J. Fernández. Effect of ZrO_2 nanoparticles on thermophysical and rheological properties of three synthetic oils. J. Mol. Liq., 2018, 262, p. 126-138
DOI: https://doi.org/10.1016/j.molliq.2018.04.027

[3] M.J.G. Guimarey, M.J.P. Comuñas, E.R. López, A. Amigo, J. Fernández. Thermophysical properties of polyalphaolefin oil modified with nanoadditives. J: Chem. Thermodyn, 2019, 131, p. 192–205
DOI: https://doi.org/10.1016/j.jct.2018.10.035

Papers soon submitted for publication:

[4] M.J.G. Guimarey, J.M. Liñeira del Río, M. Piñeiro Fiel, E.R. López, M.J.P. Comuñas, D. Cabaleiro, L. Lugo, J. Fernández. Zirconia nanoparticles as additives for trimethylolpropane trioleate based lubricants.

[5] M.J.G. Guimarey, D.E.P. Gonçalves, J.M. Liñeira del Río, M.J.P. Comuñas, J. Fernández, J.H.O. Seabra. Lubricant Properties for Nanolubricants based on Trimethylolpropane Trioleate and GnP and BN Nanoparticles.

Parts of the work contained in this thesis have been presented at conferences and can be found in the related proceedings:

[6] M.J.G. Guimarey, M.J.P. Comuñas, E.R. López, A. Amigo, J. Fernández. Study of Thermophysical Properties of Polyalphaolefin Based Nano-Lubricants. Abstract book of XV Encuentro Inter-Bienal del Grupo Especializado de Termodinámica (GET), Huelva (Spain), 2016.

[7] M.R. Salgado, M.J.G. Guimarey, M.J.P. Comuñas, E.R. López, A. Amigo, D. Cabaleiro, L. Lugo, J. Fernández. Effect of ZrO_2 Nanoparticles on Thermophysical and Rheological Properties of Synthetic Oils. Abstract book of XV Encuentro Inter-Bienal del Grupo Especializado de Termodinámica (GET), Huelva (Spain), 2016.

[8] M. Piñeiro Fiel, E.R. López, M.J.G. Guimarey, J.M. Liñeira del Río, M.J.P. Comuñas, M. Reichelt, J.Fernández. Tribological properties of trimethylolpropane trioleate-zirconia based nanolubricants. Abstract book of IX Iberian Conference on Tribology, Guimarães, (Portugal), 2017.

[9] M.J.P. Comuñas, E.R. López, A. Amigo, M.J.G. Guimarey, J.M. Liñeira del Río, J. Fernández. Desarrollo de lubricantes basados en nanoaditivos para la producción de energías renovables y uso eficiente de la energía. Abstract book of XXXVI Reunión Bienal de la Real Sociedad Española de Física, Santiago de Compostela (Spain), 2017.

[10] M.J.G. Guimarey, M.J.P. Comuñas, E.R. López, A. Amigo, J. Fernández. Densidad hasta 120 MPa y magnitudes derivadas de una polialfaolefina, PAO6. Abstract book of XXXVI Reunión Bienal de la Real Sociedad Española de Física, Santiago de Compostela (Spain), 2017.

[11] J.M. Liñeira del Río, M.J.G. Guimarey, M.J.P. Comuñas, J. Fernández. Analysis of the high pressure viscosity of trioctyl trimellitate and trimethylolpropane trioleate. Abstract book of 21st European Conference on Thermophysical Properties. Graz, (Austria), 2017

[12] M.J.G. Guimarey, M.R. Salgado, M.J.P. Comuñas, E.R. López, A. Amigo, D. Cabaleiro, L. Lugo, J. Fernández. Caracterización termofísica y reológica de nanolubricantes basados en nanopartículas de óxido de zirconio. Abstract book of VI Encontro da Mocidade Investigadora – Ciencias. Santiago de Compostela (Spain), 2018.

[13] E.R. López, M.J.G. Guimarey, O. Fandiño, M.J.P. Comuñas, J. Fernández. On the Thermodynamic Properties of Compressed Liquids using Scaling Based Eos Isobaric Heat Capacity of Eight Ionic Liquids with Potential Use as Lubricants. Abstract book of 8th International Seminar on Thermodynamic Engineering of Fluids. Tarragona (Spain), 2018.

[14] M.J.G. Guimarey, M.J.P. Comuñas, E.R. López, A. Amigo, J. Fernández. Caracterización y Propiedades Termofísicas de Nanolubricantes Basados en Nitruro de Boro y Polialfaolefinas. Abstract book of XVI Encuentro Inter-Bienal del Grupo Especializado de Termodinámica (GET). A Coruña (Spain), 2018.

Other publication on nanofluids:

[15] M.A. Marcos, D. Cabaleiro, M.J.G. Guimarey, M.J.P. Comuñas, L. Fedele, J. Fernández, L. Lugo. PEG 400-Based Phase Change Materials Nano-Enhanced with Functionalized Graphene Nanoplatelets. Nanomaterials 2018, 8(1), p. 16.
DOI: https://doi.org/10.3390/nano8010016

[16] J.M. Liñeira del Río, M.J.G. Guimarey, M.J.P. Comuñas, E.R. López, A. Amigo, J. Fernández. Thermophysical and tribological properties of dispersions based on graphene and a trimethylolpropane trioleate oil. J. Mol. Liq., 2018, 268, p. 854-866
DOI: https://doi.org/10.1016/j.molliq.2018.07.107

[17] D. Cabaleiro, M. A. Marcos, M. J. G. Guimarey, M.J.P. Comuñas, J. Fernández, L. Lugo. Dispersiones de plaquetas de grafeno en PEG 400 para almacenamiento de energía térmica y lubricación: Análisis térmico y propiedades termofísicas, Chapter book in La investigación del Grupo Especializado de Termodinámica de las Reales Sociedades Españolas de Física y de Química, 2016, pp. 1-12.

[18] D. Cabaleiro, M. A. Marcos, M. J. G. Guimarey, M.J.P. Comuñas, J. Fernández, L. Lugo. Dispersiones de plaquetas de grafeno en PEG 400 para almacenamiento de energía térmica y lubricación: Análisis térmico y propiedades termofísicas. Abstract book of XV Encuentro Inter-Bienal del Grupo Especializado de Termodinámica (GET), Huelva (Spain), 2016.

[19] D. Cabaleiro, M. A. Marcos, M. J. G. Guimarey, M.J.P. Comuñas, J. Fernández, L. Lugo. Graphene/PEG400 Nanostructured Materials for Thermal Energy Storage and Lubrication. Thermal Analysis and Thermophysical Profile. Abstract book of NANOUPTAKE COST ACTION (CA 15119) Working Group Meeting, Castellón de la Plana (Spain), 2016.

[20] J.M. Liñeira, M.J.G. Guimarey, M.J.P. Comuñas, E.R. López, A. Amigo, J. Fernández. Propiedades termofísicas y tribológicas de nanolubricantes. Abstract book of V Encontro da Mocidade Investigadora, Santiago de Compostela (Spain), 2017.

[21] J.M. Liñeira, M.J.G. Guimarey, M.J.P. Comuñas, E.R. López, A. Amigo, J. Fernández. Caracterización termofísica de nanolubricantes basados en grafeno y trioleato de

trimetilolpropano. Abstract book of XXXVI Reunión Bienal de la Real Sociedad Española de Física, Santiago de Compostela (Spain), 2017.

[22] J.M. Liñeira, M.J.G. Guimarey, M.J.P. Comuñas, E.R. López, A. Amigo, J. Fernández. Thermophysical properties of nanolubricants based on a biodegradable oil and graphene or boron nitride. Abstract book of 21st European Conference on Thermophysical Properties. Graz, (Austria), 2017.

[23] J.M. Liñeira del Río, M.J.G. Guimarey, M.J.P. Comuñas, E.R. López, J. Fernández. Propiedades tribolóxicas de nanolubricantes de nitruro de boro en polialfaolefina. Abstract book of VI Encontro da Mocidade Investigadora – Ciencias. Santiago de Compostela (Spain), 2018.

Volumetric Behaviour of Some Motor and Gear-Boxes Oils at High Pressure: Compressibility Estimation at EHL Conditions

This article deals with thermophysical characterization under high pressure of six lubricants. The analysed oils were four synthetic bases (Group I, Group III, Group IV (PAO6) and Group V) and two formulated lubricants (a gear oil and motor oil). Density data up to 120 MPa, in the temperature range from 278.15 K to 398.15 K, were reported. Among all measured lubricants, G-V has the highest densities and PAO6 was the lowest ones. The two formulated oils density values vary around 1 % over all temperature range at atmospheric pressure. The trend obtained for this property was $\rho_{\text{G-V}} > \rho_{\text{motor oil}} > \rho_{\text{G-I}} > \rho_{\text{G-Gear oil}} > \rho_{\text{G-III}} > \rho_{\text{PAO6}}$. G-I is the base oil with a density value closer to that of the formulated oils. In the case of speed of sound, G-I presented the highest values (around 1506 m s^{-1}) and PAO6 the lowest values (around 1466 m s^{-1}). Temperature seems to exhibit a significant influence on the speed of sound, varying around 14% over the entire temperature range for the six lubricants.

The obtained values for the viscosity index were 228, 191, 138, 137, 129 and 98 for gear oil, G-V, motor oil, PAO6, G-III and G-I, respectively. Isentropic compressibility (κ_s) was determined from Laplace equation. For this property the following trend was observed *PAO6 > G-III > Gear oil > Motor oil ≈ G-I >G-V*. The two formulated lubricants are significantly more viscous than the base oils at low temperatures, 813 mPa s and 300 mPa s at 278.15 K for motor oil and gear oil, respectively (with the exception of G-I base oil that is slightly more viscous than formulated gear oil). The viscosity behavior at 0.1 MPa was correlated using the Vogel-Fulcher-Tammann (VFT) equation. This regression reproduces the experimental values with average absolute deviations (AAD) lower than 1.3% for all base oils. The characterization of Elastohydrodynamic Lubrication (EHL) contacts requires an appropriate equation of state (EoS) for the lubricant. For this purpose, in this work the description of thermodynamic properties of compressed lubricants using scaling based EoS was also evaluated. Thus, Tammann-Tait (TT), Power-Law Density Scaling (PLDS) and General Density Scaling (GDS) EoSs were employed to describe the experimental densities at high pressure. The three equations correlate the experimental data excellently, with AADs lower or equal to 0.03%. In addition, the Dowson-Higginson (DH) and the Zhu and Wen (ZW) predictive equations were also tested. These predictive equations are currently used in numerical simulations of the EHL regime and predict the experimental densities with AADs lower than 0.5%. However, an asymptotic behavior was observed when density was plotted versus pressure for DH and ZW EoS, which is not a realistic behaviour. The prediction

ability of the five EoSs up to 3000 MPa was also evaluated, since this pressure can be reached in EHL lubrication. Derived volumetric properties, mainly isothermal compressibility, were also estimated using the five EoSs. Both DH and the ZW relationships underestimate the compressibility because of the asymptotic limited density value. However, TT, PLDS and GDS achieved more realistic extrapolated values from 120 MPa.

Effect of ZrO_2 Nanoparticles on Thermophysical and Rheological Properties of Three Synthetic Oils

This paper focuses on the thermophysical and rheological behaviour of nanolubricants based on three synthetic oils and ZrO_2 nanoparticles. Thus, a polyalkylene glycol (PAG) and two esters (TTM and BIOE) were used as base oils. All of them have been additivated with ZrO_2 nanoparticles by using the two-step method. To analyse the stability of the nanolubricants we have proposed a new method that was not previously reported, which consists in the temporal variation of refractive index. The stability achieved (~ 20 h) was enough to perform the experimental measurements. We must point out that a difficulty we have found in the experimental density determination is that the ZrO_2 nanoparticles adhered to the glass cell of the vibrating tube densimeters. This fact must be taken into account for future investigations with ZrO_2 nanoparticles and experimental devices based on glass cells. Temperature and nanoparticles concentration dependences of different thermophysical properties (density, viscosity and bulk modulus) at atmospheric pressure of six nanolubricants were analysed. Density and viscosity of all nanolubricants increased with the mass concentration of ZrO_2 nanoparticles and decreased with the rise of temperature. For instance, the addition of 2 wt% ZrO_2 nanoparticles caused an increase on the density of the three base oils around 1.8%. Temperature dependence of the viscosity was stronger for TTM and BIOE than PAG2. A diminution around 330 mPa s was found for PAG2 over the entire temperature range, being this value around 6500 and 5500 mPa s for TTM and BIOE, respectively. Nanoparticles concentration dependence of the viscosity provoked a higher increment for TTM based nanolubricants. The increase over all the temperature interval was found around (6 – 8) %, (4 – 5) % and (3 – 4) % for TTM, PAG2 and BIOE nanolubricants, respectively. The following sequence was obtained for the bulk modulus (K_s): *BIOE* > *TTM* > *PAG2*. Thus, nanolubricants based on PAG2 will present better low temperature fluidity.

Shear stress was measured at different shear rates for the three synthetic oils and all the nanolubricant samples. The Newtonian behavior was confirmed for the base oils and for the nanolubricants up to 10000 s^{-1} and 1000 s^{-1}, respectively. Finally, different theoretical

equations were used to estimate the above mentioned termophysical properties (viscosity and density). Densities predicted with Pak and Cho and Wasp *et al*. equations agree well with experimental values, showing AADs lower than 0.08% and 0.12% for all nanolubricants, respectively. The viscosity results obtained from predictive equations reasonably agree with the experimental viscosity data. No better agreement has been obtained because most models do not include the effects of packing fraction within the aggregates structure of additives. The best results were obtained with the Chen *et al*. model with AADs ranging from (0.29 to 0.33%), (2.27 to 3.52%) and (0.50 to 1.54%) for PAG2, TTM and BIOE based nanolubricants, respectively.

Thermophysical Properties of Polyalphaolefin Oil Modified with Nanoadditives

In this publication, thermophysical properties (viscosity, volumetric behaviour and coefficient of adiabatic compressibility) of nanolubricants based on a polyalphaolefin base oil (PAO6) and three different nanoadditives (ZrO_2 and BN nanoparticles and GnP nanoplatelets) were studied. ZrO_2 nanoparticles present a monoclinic crystal phase, BN nanoparticles have a layered hexagonal structure, and GnP nanoplatelets show a multilayer laminar structure. Nine nanolubricants with different mass concentrations were prepared: 0.5 wt %, 1 wt% and 2 wt% for ZrO_2 and 0.05 wt%, 0.10 wt% and 0.25 wt% for BN and GnP nanoadditives. Nanolubricants based on GnP were prepared using an ultrasonic bath to avoid damaging its laminar structure. No existence of new chemical bond formation between nanoparticles and base oils was observed. The temporal stability is better for graphene nanoplatelets based nanolubricants. Thus, for 0.25 wt% GnP/PAO6 nanolubricant six hours after its preparation, the refractive index variation was around 0.0002, whereas for 0.25 wt% BN/PAO6 and 2 wt% ZrO_2/PAO6 this value was 0.0004 and 0.02, respectively. The stability achieved was much higher than the time necessary to perform the experimental measurements. Density, viscosity and viscosity index at atmospheric pressure of the nanolubricants and the base oil were measured from (278.15 to 373.15) K. An increase around 0.5% on the density was observed when 0.5 wt% ZrO_2 was used. This increase is twice than that obtained when 0.25 wt% of GnP or BN is used. Therefore, no influence was found on the density produced by the shape, morphology or chemical structure of the nanoadditives.

Speed of sound at atmospheric pressure has also been determined in a temperature range from (283.15 to 343.15) K. We observe that the pressure-viscosity coefficient obtained

from Mia and Ohno method for polyalphaolefins increase with their branching degree ($\alpha_{PAO40} > \alpha_{PAO32} > \alpha_{PAO6}$). Viscosity values were successfully correlated with the Andrade´s equation, with average relative deviations lower than 0.5% for ZrO_2 and BN based nanolubricants and 0.4% for nanolubricants of GnP. It was observed a greater influence of the nanoadditives mass concentration on the viscosity than on the density. Moreover, the laminar shape of GnP nanoadditives provoked a higher increase on the viscosity than spherical shape (ZrO_2) and rod-like shape (BN) nanoparticles. Viscosity index (VI) does not present a regular dependence with the nanoparticle mass concentration. Thus, a linear dependence was only obtained for the nanolubricants formulated with BN nanoadditives. The predictive density models (Wasp *et al*. and Pak and Cho) showed a good agreement with the experimental density data. An underestimation of the density values was observed for these models. The best agreement with the experimental viscosity data was obtained for the predictive viscosity equations which includes the effects of packing fraction within the aggregates structure of additives (Chen *et al*. and Wang *et al*). Besides, the highest deviations were obtained when laminar shape nanoadditives (GnP) were used because the predictive viscosity models consider spherical particles. A successful ability of the different predictive models to estimate densities and viscosities of these nanolubricants as a function of temperature and nanoparticle concentration was observed.

Zirconia Nanoparticles as Additives for Trimethylolpropane Trioleate Based Lubricants

This article focuses on the analysis of tribological performance (anti-friction properties and anti-wear capability), thermal and rheological behavior of nanolubricants composed by an ester synthetic oil, trimethylolpropane trioleate (TMPTO), and nanoparticles of zirconium oxide (ZrO_2). Stable homogeneous nanolubricants of ZrO_2 nanoparticles in TMPTO (at 0.25, 0.5, 0.75 and 1.0 wt% mass concentrations) were prepared without any surfactant by using an ultrasonic disruptor. The nanolubricants stability was checked by means of DLS analysis that allows to control the nanoparticles sedimentation or aggregation from the measurements of the average particle size (APS). The APS obtained from DLS analysis was found around 450 nm. Thus, the predominant mechanism observed was nanoparticle aggregation. Thermal conductivity and rheological behaviour of neat base oil and 0.5 wt% and 1.0 wt% ZrO_2 based nanolubricants were measured. The thermal conductivity test showed a linear dependence with nanoparticle mass concentration.

A slightly non-Newtonian behavior was detected at low shear rates and temperatures for 0.5 wt% and 1.0 wt% ZrO_2 nanolubricants. Tribological essays were carried out with the base oil and the nanolubricants using a reciprocating ball-on-plate tribometer at room temperature conditions under workloads of 2.5 and 5.0 N. A reduction of the friction coefficient was observed for all the nanolubricants. Nevertheless, only wear enhancement was observed for 0.25 wt% of ZrO_2 nanolubricant under 2.5 N load. In this case, the width of track wear (WTW) was 591 nm and 585 nm for pure TMPTO and for 0.25 wt% of ZrO_2 nanolubricant, respectively. The wear was produced by plastic deformation and abrasion. For TMPTO base oil the roughnesses of the worn surface, *Ra*, were 78 nm and 187 nm under loads of 2.5 N and 5 N, respectively. For 0.25 wt% nanolubricant based on ZrO_2, the roughnesses were 101 nm and 214 nm at the same loads, respectively. SEM images and roughness analysis of the worn surface formed on the test specimens (plates) showed abrasion during the tribotests when the nanoparticle concentration rise. Thus, the abrasion inhibited the anti-wear effect of the nanoparticles. The best antifriction improvement was obtained for 0.25 wt% of ZrO_2 nanolubricant under the load of 5.0 N.

Lubricant Properties for Nanolubricants Based on Trimethylolpropane Trioleate and GnP and BN Nanoparticles

In this work, determination of the film thickness and friction properties (friction coefficient and Stribeck curves) of six based on trimethylolpropane trioleate (TMPTO) nanolubricants was performed under different slide-to-roll ratios (SRR) and temperatures. Pure base oil was additivated with two different nanoadditives: boron nitride nanoparticles (BNNPs) and graphene nanoplatelets (GnPs) at 0.25, 0.5 and 1.0 wt% mass concentrations. Besides, the high-pressure density and viscous behaviour was experimentally performed for the pure base oil to obtain the viscosity-pressure coefficient, α_{film}. For BNNPs, no clear dependence between the film thickness and the mass nanoadditive concentration was observed at fixed entrainment speed. However, an increase in the film thickness was observed with the addition of GnP for the most of the entrainment speeds, temperatures and mass concentrations. For instance, a maximum increment in the film thickness (around 8%) was obtained at 2 m s^{-1} and 333.15 K for 0.25 wt% of GnP. Usually, graphene nanoplatelets have a higher influence in the film thickness than BNNPs. Density data were measured for pure TMPTO from (278.15 to 398.15) K up to 100 MPa. The density increases were around 4% and 7% over all the pressure interval at 278.15 K and 398.15 K, respectively. Density

values were correlated from Tait-like equation for the TMPTO over the entire temperature and pressure ranges, obtaining standard deviation lower than 0.9 kg m^{-3}.

The dynamic viscosity values at high pressures for TMPTO range from 15 mPa s (at 353.15 K and 10 MPa) to 521 mPa s (at 303.15 K and 150 MPa). The pressure effect on viscosity become smaller as temperature increases. Thus, at T = 303.15 K the viscosity at 150 MPa is around seven times higher than that at 10 MPa, and at 353.15 K four times higher. The pressure-viscosity coefficient (α_{film}) is calculated from Bair method using the experimental viscosity data at high pressure. For pure TMPTO, we have obtained α_{film} values of 12.5 GPa^{-1} and 10.7 GPa^{-1}at 323.15 K and 353.15 K, respectively. We have also estimated the pressure-viscosity coefficient (α_{Gold}) of the pure base oil (TMPTO) from the Gold´s equation. We observe that α_{film} values are higher than the corresponding α_{Gold} values. We have found deviations around 16% at 303.15 K, 13% at 333.15 K and 10% at 353.15K between α_{film} and α_{Gold}.

The film thickness, h_0, was estimated from both, the universal pressure-viscosity coefficient obtained from Bair method (α_{film}) and with the pressure-viscosity coefficient from the Gold´s equation (α_{Gold}). The experimental film thickness was compared with the estimated h_0 values. The absolute average deviations (AAD%) between film thickness measurements and film thickness estimated were 11.3% (303.15 K), 2.5% (333.15 K) and 2.9% (353.15 K) for Bair equation and 2.7% (303.15 K), 6.7% (333.15 K), and 9.2% (353.15 K) for Gold equation. The Gold equation underestimate the viscosity-pressure coefficient, and consequently the film thickness. The Stribeck curves for all nanolubricants and base oil were measured at temperatures of 303.15, 333.15 and 353.15 K at SRR of 5% and 50%. Different roughness discs (a polished disc and two rough discs of Ra = 0.1 μm and Ra = 0.5 μm) were used. In all the performed tests, the Stribeck curves for base oil and nanolubricants are placed between elastohydrodynamic lubrication (higher speeds) and mixed lubrication (lower speed). The maximum increase in film thickness and the lower friction coefficient, with respect to pure base oil, was obtained for the nanolubricant TMPTO/0.25 wt% GnP under a SRR of 5% at all temperatures.

M.J.G. Guimarey, M.J.P. Comuñas, E.R. López, A. Amigo, J. Fernández, Volumetric Behavior of some Motor and Gear-Boxes Oils at High Pressure: Compressibility Estimation at EHL Conditions, Ind. Eng. Chem. Res. 56 (2017) 10877–10885

DOI: 10.1021/acs.iecr.7b02002

M.J.G. Guimarey, M.R. Salgado, M.J.P. Comuñas, E.R. López, A. Amigo, D. Cabaleiro, L. Lugo, J. Fernández, Effect of ZrO_2 Nanoparticles on Thermophysical and Rheological Properties of Three Synthetic Oils, J. Mol. Liq. 262 (2018) 126-138

DOI: https://doi.org/10.1016/j.molliq.2018.04.027

M.J.G. Guimarey, M.J.P. Comuñas, E.R. López, A. Amigo, J. Fernández, Thermophysical Properties of Polyalphaolefin Oil Modified with Nanoadditives, J. Chem. Thermodyn, 131 (2019) 192–205

DOI: https://doi.org/10.1016/j.jct.2018.10.035

Artículo pendiente de publicación:

Zirconia Nanoparticles as Additives for Trimethylolpropane Trioleate Based Lubricants

Artículo pendiente de publicación:

Lubricant Properties for Nanolubricants Based on Trimethylolpropane Trioleate and GnP and BN Nanoparticles

USC
UNIVERSIDADE
DE SANTIAGO
DE COMPOSTELA

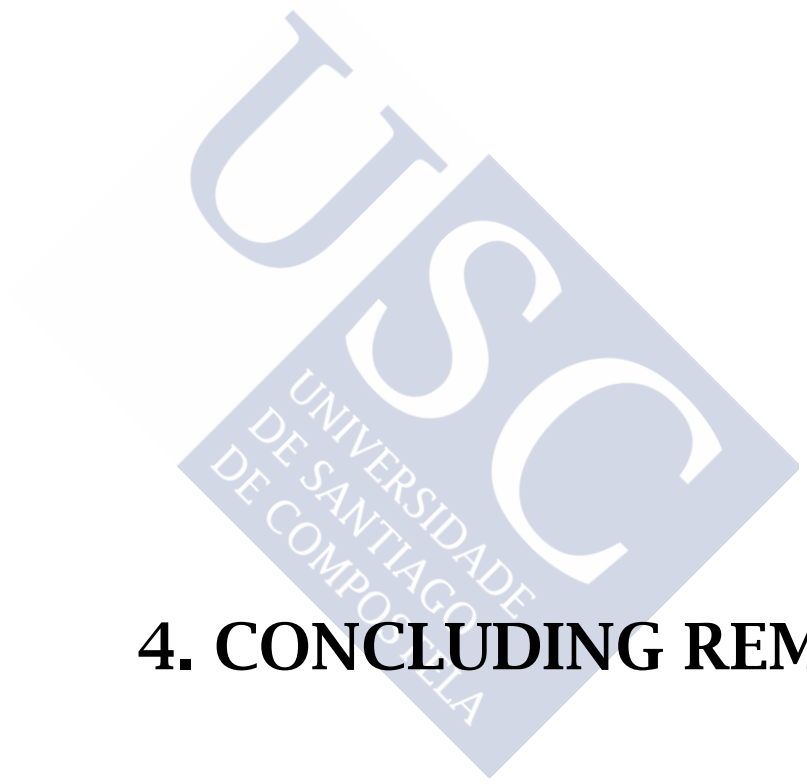

4. CONCLUDING REMARKS

USC
UNIVERSIDADE
DE SANTIAGO
DE COMPOSTELA

4. CONCLUDING REMARKS

This PhD Thesis was carried out under the framework of two larger national research projects focused on the characterization and develop of nanolubricants for several applications in renewable energy and automotive systems. The main findings of this work are:

- A new method to control the sedimentation rate in nanolubricants was proposed and rigorously checked. This method is based on the temporal evolution of the refractive index.
- Dynamic Light Scattering (DLS) data show agglomeration of ZrO_2 nanoparticles for nanolubricants based on PAG2, TTM, BIOE and TMPTO. The average cluster size of these nanolubricants has the following trend with the base oil: *TMPTO > PAG2 > TTM > BIOE*. The nanolubricant based on TMPTO revels the highest average cluster size, which is around ten times those of the ZrO_2 nanoparticles.
- The sedimentation of ZrO_2 nanoparticles is faster in PAO6 than in polyalkyleneglycol, polymeric ester, isotridecyl trimellitate or trimethylolpropane trioleate base oils. GnP nanoadditives lead to PAO6 based nanolubricants with slightly better stability than ZrO_2 and BN nanoparticles.
- The shorter stability of the designed nanolubricants did not affect thermophysical property measurements: viscosity index, density, dynamic viscosity, speed of sound, flow properties and thermal conductivity. Thus, no fluctuations were observed during the experiments.
- The ZrO_2 nanoparticles were adhered to the glass cell of the vibrating tube densimeters. This fact must be taken into account for future investigations with ZrO_2 nanoparticles and experimental devices based on glass cells.
- Viscosity indexes of PAO6/ZrO_2, PAO6/BN and PAO6/GnP nanolubricants have not a regular dependence with the mass concentration of nanoadditives.
- The thermal conductivity of nanolubricant based on TMPTO with 0.5 wt% and 1.0 wt% of ZrO_2 decreases when temperature rises and shows a practically linear relation with nanoparticle concentration.
- Nanolubricants based on ZrO_2 nanoparticles exhibited non-Newtonian behavior at low temperatures and low shear rates when TMPTO was used as base oil. However, a linear relationship in the flow curves was found for the nanolubricants based on PAG2, TTM and BIOE with ZrO_2 nanoparticles up to shear rates of 1000 s^{-1}.

- Models considering the effects of packing fraction within the aggregate structure of additives predict better the viscosity of nanolubricants based on PAG2, TTM, BIOE and PAO6.
- The influence of different morphology and concentration nanoparticles was studied using ZrO_2, BN and GnP nanoadditives. The presence of these nanoadditives has stronger effect on the viscosity than on the density of PAO6, TTM, PAG2 and BIOE based nanolubricants.
- The dispersion of nanoadditives with laminar shape provokes a larger increase on the viscosity of the polyalphaolefin base oil than those with spherical or rod-like morphologies.
- Density of six lubricants were measured in the temperature range from 278.15 K to 398.15 K up to 120 MPa with a high pressure vibrating tube densimeter. Data were correlated as a function of temperature and pressure through three equations of state, Tammann-Tait equation, power-law density scaling (PLDS) and general density scaling (GDS), all with an absolute average deviation lower or equal to 0.03%. PAO6 is the most expandable oil, except for pressures higher than 60 MPa for which it is G-V. Thus, the isobaric thermal expansion coefficient of these lubricants presents the following trends at low pressures: *PAO6 > gear oil ≈ G-III > G-V > motor oil > G-I*, and at high pressures: *G-V > PAO6 > gear oil ≈ G-III > motor oil > G-I*.
- Tribological analysis of zirconia nanolubricants based on TMPTO show that the best antifriction behavior (49% enhancement) was obtained under the load of 5.0 N for the nanolubricant containing 0.25 wt% of ZrO_2. The wear was not improved with the addition of nanoparticles. Thus, under a load of 2.5 N a higher abrasion was observed when the nanoparticles concentration increases.
- The film thickness was studied for trimethylolpropane trioleate (TMPTO) and six different nanolubricants formulated with BNNPs and GnP nanoadditives. A relative deviation around 11% (at 303.15 K) and 3% (at 353.15 K) was observed between the film thickness experimentally determined by optical interferometry and that obtained from Hamrock and Dowson equation (using high-pressure viscosity data). The addition of nanoparticles into the base oil did not reveal a clear relationship between the film thickness and the nanoparticle mass concentration. The graphene nanoplatelets have a higher influence in the film thickness than boron nitride nanoparticles.

- The friction properties of TMPTO and nanolubricants formulated with this base oil and BNNPs and GnP nanoadditives were studied under different, slide-to-roll ratios (SRR) and temperatures. All friction tests were performed under elastohydrodynamic and mixed lubrication regimes for all testing conditions. The maximum increase in film thickness and the lower friction coefficient, with respect to pure base oil, was obtained for TMPTO/0.25 wt% GnP under a SRR of 5% at all temperatures.

USC
UNIVERSIDADE
DE SANTIAGO
DE COMPOSTELA

5. APPENDIX

USC
UNIVERSIDADE
DE SANTIAGO
DE COMPOSTELA

Resumen

El control y la optimización de la lubricación tiene una gran importancia desde el punto de vista económico. Los lubricantes son una poderosa herramienta para la tribología porque realizan una serie de funciones críticas: lubricación, refrigeración y protección de superficies metálicas entre otras. Para seleccionar el tipo de lubricante se deben tener en cuenta varios factores: el rango de temperatura, la velocidad, la carga, los materiales de las superficies de contacto, así como consideraciones generales del diseño de la propia máquina. La necesidad de desarrollar nuevos lubricantes con mejores propiedades antifricción y antidesgaste se justifica por el ahorro energético que esto implicaría. En general, un lubricante se formula a partir de aceites base a los que se les añaden aditivos apropiados para obtener un rendimiento óptimo. Los aceites base se clasifican en tres categorías según el proceso de obtención: aceites minerales, sintéticos y vegetales. Un lubricante contiene generalmente alrededor del 93% de aceites base y el 7% de aditivos químicos. Los aditivos son compuestos orgánicos o inorgánicos disueltos o suspendidos en el aceite base. La idea de usar nanopartículas como aditivos antifricción y antidesgaste se ha convertido en un campo de investigación interesante en los últimos años. Las principales ventajas del uso de nanopartículas son: la baja interacción con otros aditivos; su capacidad para formar películas sobre las superficies y su resistencia a altas temperaturas.

Para proponer nuevos nanolubricantes es de vital importancia analizar el efecto que tiene la adición de los nanoaditivos en sus propiedades termofísicas, ya que también afectan a su rendimiento final. El conocimiento de la viscosidad y del comportamiento reológico es importante en el diseño de un sistema mecánico lubricado. Además, la viscosidad es clave en el sellado y en la tasa de consumo de aceite, de la misma manera, optimiza las condiciones de arranque y el funcionamiento de las máquinas en condiciones de temperatura variable. Por lo tanto, una alteración fuerte de esta propiedad puede causar fallos en el sistema de bombeo. La conductividad térmica es esencial para evaluar el efecto del calentamiento en la lubricación y en el diseño de rodamientos. Además, debido a la presión de trabajo existente en los rodamientos, el cambio de la densidad con la presión es esencial en contactos lubricados que operan a altas cargas. Para la aplicación de nanolubricantes también es necesario conocer mejor el mecanismo que controla su rendimiento tribológico. El comportamiento termofísico y tribológico depende de varios factores, como el aceite base utilizado para la formulación del nanolubricante, el tamaño, la forma y la concentración de las nanopartículas, junto con la temperatura y la presión de funcionamiento de la maquinaria para la cual se desarrolla el nanolubricante.

Esta Tesis Doctoral se centra en el análisis de las propiedades termofísicas y tribológicas de aceites base, aceites comerciales y nanolubricantes. Los aceites estudiados son sintéticos, ocho de ellos son aceites base y dos de ellos lubricantes comerciales. Estos aceites han sido suministrados por las empresas Croda, Verkol y Repsol, que colaboran en los dos proyectos nacionales de investigación NanoLuter y AdLuter en los que se enmarca esta Tesis Doctoral. En concreto se han utilizado cuatro ésteres: trimetilolpropano trioleato (TMPTO), isotridecil trimelitato (TTM), un éster polimérico biodegradable (BIOE) y una mezcla de dos ésteres, trimetilolpropano y neopentilglicol. Este último fluido se denomina (G-V) debido a que se engloba en el grupo V de la clasificación propuesta por el American Petroleum Institute (API). Los otros aceites sintéticos son: un polialquilenglicol (PAG2), una polialfaolefina (PAO6) clasificada en el grupo IV de la API (G-IV), un aceite parafínico (SN-230) clasificado en el grupo I (G-I) y un aceite (hydrocracking oil) del grupo III (G-III). Además, también se estudiaron dos lubricantes comerciales sintéticos, un aceite de caja de engranajes (75W40) y un aceite de motor (15W40).

Las nanopartículas que se utilizaron como aditivos han sido suministradas por la empresa Iolitec y tienen distinta morfología: nanopartículas de óxido de zirconio (ZrO_2), de nitruro de boro (BN) y nanoplaquetas de grafeno (GnP). El ZrO_2 tiene un diámetro nominal de (30-60) nm y una densidad aparente de 5.9 g cm^{-3}. Las nanopartículas de nitruro de boro (BN) un diámetro nominal de 70 nm y una densidad aparente de 2.29 g cm^{-3}. Las nanoplaquetas de grafeno (GnP) tienen un tamaño medio de (11–15) nm y una densidad aparente de 2.25 g cm^{-3}. Para caracterizar tanto los aceites base como las nanopartículas se han empleado diferentes técnicas: espectrometría de masas, resonancia magnética nuclear (NMR), microscopía electrónica de barrido (SEM), microscopía electrónica de transmisión (TEM), espectroscopia Raman y difracción de rayos X (XRD). Estos experimentos se realizaron en colaboración con el Servicio de Apoyo a la Investigación (RIAIDT) de la Universidad de Santiago de Compostela.

En esta Tesis Doctoral se ha utilizado el método de dos pasos para preparar los nanolubricantes. La concentración de masa de ambos componentes (aceite base y nanopartículas) se ha determinado utilizando una microbalanza Sartorius MC 210P de alta precisión. Para dispersar las nanopartículas en el aceite base, se han empleado una punta de ultrasonidos (HD 2200 Sonopuls) y un baño de ultrasonidos (Fisherbrand). La energía transferida al nanolubricante cuando se emplea la punta depende de la potencia aplicada, del tiempo total de sonicación, del volumen de la muestra, de la forma y del diámetro de la sonda y de la profundidad de inmersión. Las condiciones de sonicación utilizadas en esta tesis han

sido: potencia (200W), amplitud (302 μm), tipo de sonda y diámetro (MS73, 3 mm) y tiempo de sonicación (30 min). Para minimizar el sobrecalentamiento durante el proceso de sonicación las muestras se sumergieron en un baño de hielo. El baño de ultrasonidos se ha empleado principalmente para preparar nanolubricantes que contienen nanoplaquetas de grafeno. Se han utilizado las siguientes condiciones: períodos de agitación continua de 2 h, una potencia efectiva de 180 W y una frecuencia de agitación de 37 kHz. Otro equipo que se ha empleado para dispersar los nanolubricantes es un agitador mecánico Fisherbrand Vortex. Las muestras se han agitado durante 10 minutos a 16 rpm. Para analizar la estabilidad de los nanolubricantes formulados se emplearon varios métodos: control visual, espectrofotometría UV-Vis y dispersión de luz dinámica (DLS). También se ha analizado, por primera vez, el uso de un turbidímetro para controlar la estabilidad. Finalmente, se ha propuesto un nuevo método para controlar la sedimentación basado en la evolución temporal del índice de refracción.

El comportamiento volumétrico y viscoso, el índice de viscosidad, las curvas de flujo y la conductividad térmica de los aceites base, los lubricantes comerciales y los nanolubricantes se determinaron experimentalmente empleando densímetros de tubo vibrante a presión atmosférica y a alta presión, un viscosímetro rotacional y un reómetro con geometría cono-plato. Se ha realizado la caracterización termofísica a alta presión de seis lubricantes: cuatro bases sintéticas (G-I, G-III, PAO6 y G-V) y dos lubricantes comerciales (75W90 y 15W40). Se ha determinado experimentalmente la densidad hasta los 120 MPa en el rango de temperatura de 278.15 K a 398.15 K, además de la densidad, viscosidad, índice de viscosidad y velocidad del sonido desde 278.15 K hasta 373.15 K a presión atmosférica. Entre todos los lubricantes estudiados, el fluido más denso es el G-V, mientras que la PAO6 es el aceite que presenta los valores de densidad más bajos. Los dos lubricantes comerciales poseen una densidad muy parecida, con una diferencia del 1% en todo el rango de temperatura a 0.1 MPa. El incremento de la densidad con la presión es similar para los seis aceites, obteniéndose un incremento promedio del 5% para la temperatura más baja (278.15 K) y del 8% para la temperatura más alta (398.15 K). La tendencia obtenida para esta propiedad fue: $\rho_{G\text{-}V} > \rho_{15W40} > \rho_{G\text{-}I} > \rho_{75W90} > \rho_{G\text{-}III} > \rho_{PAO6}$. G-I es el aceite base con un valor de densidad más cercano al de los aceites comerciales.

En el caso de la velocidad del sonido, G-I presentó los valores más altos (alrededor de 1506 m s^{-1}) y la PAO6 los valores más bajos (alrededor de 1466 m s^{-1}). La temperatura tiene una influencia significativa en esta propiedad, observándose variaciones del 14% en todo el rango de temperatura. Los valores obtenidos para el índice de viscosidad fueron 228,

191, 138, 137, 129 y 98 para 75W90, G-V, 15W40, PAO6, G-III y G-I, respectivamente. La compresibilidad isoentrópica (κ_s) se determinó a partir de la ecuación de Laplace. Para esta propiedad se observó la siguiente tendencia: *PAO6 > G-III > 75W90 > 15W40 ≈ G-I > G-V*. Por otro lado, los dos lubricantes comerciales son significativamente más viscosos que los aceites base a bajas temperaturas, 813 mPa s y 300 mPa s a 278.15 K para 15W40 y 75W90, respectivamente. Con la excepción del aceite base G-I (367 mPa s a 278.15 K) que es ligeramente más viscoso que el 75W90. El comportamiento de la viscosidad a 0.1 MPa se correlacionó utilizando la ecuación de Vogel-Fulcher-Tammann (VFT). Esta regresión reproduce los valores experimentales con desviaciones medias absolutas (AADs) inferiores al 1.3% para todos los aceites base.

La caracterización de los contactos de lubricación elastohidrodinámica (EHL) requiere una ecuación de estado (EoS) adecuada para el lubricante. Para este propósito se han empleado las EoS de Tammann-Tait (TT), Power-Law Density Scaling (PLDS) y General Density Scaling (GDS) para describir las densidades experimentales a alta presión. Estas tres ecuaciones correlacionan de manera excelente los datos experimentales, con AADs menores o iguales a 0.03%. Además, también se aplicaron las ecuaciones predictivas de Dowson-Higginson (DH) y Zhu y Wen (ZW). Estas ecuaciones predicen las densidades experimentales con AADs inferiores al 0.5%. Sin embargo, se observa un comportamiento asintótico cuando se representa la densidad en función de la presión para las EoS de DH y ZW. Se ha evaluado la capacidad de predicción de las cinco EoS hasta 3000 MPa, ya que esta presión puede alcanzarse en el régimen EHL. También se han estimado propiedades volumétricas derivadas, principalmente la compresibilidad isotérmica.

Se ha estudiado el comportamiento termofísico y reológico de nanolubricantes formulados con nanopartículas de ZrO_2 a partir de tres aceites sintéticos: un polialquilenglicol (PAG) y dos ésteres (TTM y BIOE). Para los nanolubricantes, se analizaron las dependencias con la temperatura y con la concentración de nanopartículas de diferentes propiedades termofísicas (densidad, viscosidad y velocidad del sonido) a presión atmosférica. Se observó que la densidad y la viscosidad de todos los nanolubricantes aumenta con la concentración de las nanopartículas de ZrO_2 y disminuye con el aumento de la temperatura. Por ejemplo, la adición de 2% en peso de nanopartículas de ZrO_2 provoca un aumento en la densidad de los tres aceites base del 1.8%. La dependencia de la viscosidad con la temperatura es mayor para los nanolubricantes basados en TTM y BIOE que para los formulados a partir de PAG2. La dependencia de la viscosidad con la concentración de nanopartículas es mayor para los nanolubricantes basados en TTM. El aumento en todo el

intervalo de temperatura es del (6-8)%, (4-5)% y (3-4)% para los nanolubricantes de TTM, PAG2 y BIOE, respectivamente. Se ha obtenido la siguiente secuencia para el módulo de compresibilidad (K_s): *BIOE> TTM> PAG2*. Por lo tanto, los nanolubricantes basados en PAG2 presentarán una mejor fluidez a baja temperatura.

Las curvas de flujo se determinaron para los tres aceites sintéticos y todos los nanolubricantes. Se confirmó el comportamiento newtoniano para los aceites base y para los nanolubricantes hasta velocidades de deformación de 10000 s^{-1} y 1000 s^{-1}, respectivamente. Finalmente, se utilizaron diferentes ecuaciones teóricas para predecir las propiedades termofísicas de nanolubricantes a partir de las propiedades de los aceites base y de las nanopartículas. Los resultados de densidad obtenidos con las ecuaciones de Pak y Cho y Wasp *et al*. están de acuerdo con los valores experimentales, obteniéndose AADs inferiores al 0.08% y 0.12% para todos los nanolubricantes, respectivamente. Las viscosidades obtenidas a partir de las ecuaciones predictivas concuerdan razonablemente bien con los datos de viscosidad experimentales. Los mejores resultados se obtuvieron con la ecuación de Chen *et al*. con AADs variando entre (0.29 y 0.33%), (2.27 y 3.52%) y (0.50 y 1.54%) para nanolubricantes basados en PAG2, TTM y BIOE, respectivamente. También se ha analizado la conductividad térmica y el comportamiento reológico del aceite base puro TMPTO y de los nanolubricantes formulados con un 0.5% y un 1.0% en peso de ZrO_2. La conductividad térmica mostró una dependencia lineal con la concentración en peso de las nanopartículas. En cuanto al estudio reológico, se detectó un comportamiento ligeramente no newtoniano a bajas velocidades de cizallamiento y a bajas temperaturas para ambos nanolubricantes.

Se han estudiado las propiedades termofísicas (viscosidad, comportamiento volumétrico y coeficiente de compresibilidad adiabático) de los nanolubricantes basados en una polialfaolefina (PAO6) y tres nanoaditivos diferentes (nanopartículas de ZrO_2 y BN y nanoplaquetas GnP). Se prepararon nueve nanolubricantes con diferentes concentraciones en peso: 0.5%, 1.0% y 2.0% para ZrO_2 y 0.05%, 0.10% y 0.25% para BN y GnP. El índice de viscosidad, densidad y viscosidad a presión atmosférica de los nanolubricantes y del aceite base se ha medido desde 278.15 K hasta 373.15 K. Se observó un aumento del 0.5% en la densidad para el nanolubricante que contiene un 0.5% en peso de ZrO_2. Este aumento es el doble que el obtenido con un 0.25% en peso de GnP o BN. Por lo tanto, no se observa a priori una influencia significativa de la forma, morfología o estructura química de los nanoaditivos sobre la densidad.

La velocidad del sonido a presión atmosférica también se ha determinado en un rango de temperatura de 283.15 K a 338.15 K. Se ha observado que el coeficiente de viscosidad-presión obtenido a partir de la ecuación propuesta por Mia y Ohno para polialfaolefinas aumenta con el grado de ramificación de las PAOs ($\alpha_{PAO40} > \alpha_{PAO32} > \alpha_{PAO6}$). Los valores de viscosidad se correlacionaron con éxito mediante la ecuación de Andrade, con desviaciones relativas inferiores al 0.5% para nanolubricantes formulados con ZrO_2 y BN y 0.4% para nanolubricantes con GnP. Se observó una mayor influencia de la concentración de los nanoaditivos en la viscosidad que en la densidad. Además, la forma laminar de los nanoaditivos de GnP provocó un aumento mayor en la viscosidad que el producido por las nanopartículas esféricas (ZrO_2) y rod-like (BN). El índice de viscosidad (VI) no presenta una dependencia regular con la concentración en peso de las nanopartículas. Solo se obtuvo una dependencia lineal para los nanolubricantes formulados con nanoaditivos de nitruro de boro. Los modelos predictivos de Wasp *et al*. y Pak y Cho subestiman ligeramente la densidad de los nanolubricantes. El mejor acuerdo entre la predicción y los valores experimentales de viscosidad se obtuvo para los nanolubricantes formulados con ZrO_2 (forma esférica), mientras que las desviaciones más altas se obtuvieron con nanoaditivos con estructura laminar (GnP), esto se debe a que estos modelos consideran las nanopartículas esféricas.

En lo que respecta al comportamiento tribológico este trabajo se ha centrado en el estudio del coeficiente de viscosidad-presión para la lubricación elastohidrodinámica, en el espesor de película, en el desgaste y en el coeficiente de fricción. Estas propiedades se obtuvieron empleando un viscosímetro de caída de cuerpo a alta presión, un tribómetro de bola sobre disco equipado con interferometría óptica, un perfilómetro óptico 3D y un tribómetro con configuración de bola sobre placa y movimiento reciprocante. Se ha estudiado el comportamiento tribológico (propiedades antifricción y capacidad antidesgaste) de los nanolubricantes compuestos por trioleato de trimetilolpropano (TMPTO) y nanopartículas de óxido de zirconio (ZrO_2). Las concentraciones estudiadas han sido: 0.25, 0.5, 0.75 y 1.0% en peso. Los ensayos tribológicos se llevaron a cabo con el aceite base y los nanolubricantes utilizando un tribómetro con configuración de bola sobre placa a temperatura ambiente con cargas de trabajo de 2.5 y 5.0 N. Se observó una reducción del coeficiente de fricción para todos los nanolubricantes. Sin embargo, el desgaste sólo mejoró para el nanolubricante de 0.25% en peso de ZrO_2 para la carga de 2.5 N. En este caso, se obtuvo un ancho de la huella de desgaste de 591 nm y 585 nm para el TMPTO puro y para el nanolubricante de 0.25% en peso de ZrO_2, respectivamente. Para el aceite base TMPTO,

se han obtenido rugosidades de la superficie desgastada, *Ra*, de 78 nm y 187 nm para cargas de 2.5 N y 5 N, respectivamente. Para el nanolubricante formulado con un 0.25% en peso de ZrO_2, las rugosidades obtenidas son mayores, 101 nm y 214 nm para las mismas cargas, respectivamente. Las imágenes SEM y el análisis de rugosidad de la superficie realizados en la zona desgastada de las placas, ponen de manifiesto la existencia de abrasión, la cual inhibe el efecto antidesgaste de las nanopartículas. El menor coeficiente de fricción se ha obtenido para el nanolubricante de 0.25% en peso de ZrO_2 sometido a la carga de 5.0 N.

La determinación del espesor de película y de las propiedades de fricción (coeficiente de fricción y curvas de Stribeck) de seis nanolubricantes basados en trioleato de trimetilolpropano (TMPTO) se ha realizado para diferentes condiciones de deslizamiento-rodadura (SRR) y de temperatura. El TMPTO se aditivó con nanopartículas de nitruro de boro (BNNPs) y nanoplaquetas de grafeno (GnPs) a concentraciones de 0.25, 0.5 y 1.0% en peso. Para las BNNPs, no se ha observado una clara dependencia entre el espesor de película y la concentración de nanopartículas a una velocidad de arrastre fija. Sin embargo, si se observó un aumento en el espesor de película con la adición de GnP para la mayoría de las velocidades, temperaturas y concentraciones. Por ejemplo, se obtuvo un incremento máximo en el espesor de película (alrededor del 8%) a 2 m s^{-1} y 333.15 K para el nanolubricante que contiene 0.25% en peso de GnP. En general, los resultados obtenidos parecen poner de manifiesto que las nanoplaquetas de grafeno tienen una mayor influencia en el espesor de película que las nanopartículas de nitruro de boro.

Además, se ha determinado experimentalmente la densidad y viscosidad a alta presión del TMPTO puro para poder obtener el coeficiente de viscosidad-presión. Los datos de densidad para el TMPTO se midieron en el rango de temperaturas entre 278.15 K y 398.15 K hasta 100 MPa. Los aumentos de densidad son del 4% y 7% en todo el intervalo de presión a 278.15 K y 398.15 K, respectivamente. Los valores de densidad para el TMPTO se correlacionaron con una ecuación de tipo Tait, obteniéndose una desviación estándar inferior a 0.9 kg m^{-3}. Los valores de viscosidad a altas presiones para el TMPTO varían desde 15 mPa s (a 353.15 K y 10 MPa) hasta 521 mPa s (a 303.15 K y 150 MPa). El coeficiente de viscosidad-presión (α_{film}) se calculó a partir del método propuesto por Bair usando los datos de viscosidad a alta presión. Para el TMPTO puro, se han obtenido valores de α_{film} de 12.5 GPa^{-1} y 10.7 GPa^{-1} a 323.15 K y 353.15 K, respectivamente. El espesor de película, h_0, se estimó a partir del coeficiente de viscosidad-presión universal obtenido mediante el método de Bair (α_{film}) y a partir del coeficiente de viscosidad-presión obtenido con la ecuación de Gold (α_{Gold}). Las desviaciones promedio entre los valores del espesor de película

experimental y los estimados son 11.3% (303.15 K), 2.5% (333.15 K) y 2.9% (353.15 K) para la ecuación de Bair y 2.7% (303.15 K), 6.7% (333.15 K) y 9.2% (353.15 K) para la ecuación de Gold.

Las curvas de Stribeck para todos los nanolubricantes basados en TMPTO y para el aceite base se han medido a temperaturas de 303.15, 333.15 y 353.15 K y a SRR de 5% y 50%. Se utilizaron discos con diferente rugosidad (un disco pulido y dos discos rugosos de *Ra*=0.1 μm y *Ra*=0.5 μm). Las curvas de Stribeck, tanto del aceite base como de los nanolubricantes, se sitúan entre la lubricación elastohidrodinámica EHL (velocidades más altas) y la lubricación mixta (velocidades más bajas). El mayor aumento en el espesor de película y el menor coeficiente de fricción, con respecto al aceite base puro, se obtuvo a todas las temperaturas con el nanolubricante de 0.25% en peso de GnP y una SRR de 5%.

USC
UNIVERSIDADE
DE SANTIAGO
DE COMPOSTELA